UNIVERSITÉ TOULOUSE III – PAUL SABATIER
FACULTÉS DE MÉDECINE

ANNÉE 2022 2022-TOU3-1628

THÈSE

POUR LE DIPLÔME D'ÉTAT DE DOCTEUR EN MÉDECINE SPECIALISÉE CLINIQUE

Présentée et soutenue publiquement par

Gildas GABIACHE

le 30 septembre 2022

THE ROLE OF IMAGE-GUIDED PRECISION MEDICINE IN THE DIAGNOSIS AND TREATMENT OF PHEOCHROMOCYTOMAS AND PARAGANGLIOMAS IN THE ERA OF IMAGING BIOMARKERS AND ARTIFICIAL INTELLIGENCE

Directrice de Thèse : Madame le Professeur Fatima MOKRANE

JURY

Monsieur le Professeur Hervé ROUSSEAU	Président
Madame le Professeur Fatima MOKRANE	Assesseur
Monsieur le Docteur Laurent DERCLE	Assesseur
Monsieur le Docteur Lawrence DIERICKX	Assesseur
Madame le Docteur Céline MOULY	Assesseur
Monsieur le Docteur Matthieu THOULOUZAN	Assesseur

FACULTE DE SANTE
Département Médecine Maieutique et Paramédicaux
Tableau des personnels HU de médecine
Mars 2022

Professeurs Honoraires

Doyen Honoraire	M. CHAP Hugues
Doyen Honoraire	M. GUIRAUD-CHAUMEIL Bernard
Doyen Honoraire	M. LAZORTHES Yves
Doyen Honoraire	M. PUEL Pierre
Doyen Honoraire	M. ROUGE Daniel
Doyen Honoraire	M. VINEL Jean-Pierre
Professeur Honoraire	M. ABBAL Michel
Professeur Honoraire	M. ADER Jean-Louis
Professeur Honoraire	M. ADOUE Daniel
Professeur Honoraire	M. ARBUS Louis
Professeur Honoraire	M. ARLET Philippe
Professeur Honoraire	M. ARLET-SUAU Elisabeth
Professeur Honoraire	M. ARNE Jean-Louis
Professeur Honoraire	M. BARRET André
Professeur Honoraire	M. BARTHE Philippe
Professeur Honoraire	M. BAYARD Francis
Professeur Honoraire	M. BLANCHER Antoine
Professeur Honoraire	M. BOCCALON Henri
Professeur Honoraire	M. BONAFÉ Jean-Louis
Professeur Honoraire	M. BONEU Bernard
Professeur Honoraire	M. BONNEVIALLE Paul
Professeur Honoraire	M. BOUNHOURE Jean-Paul
Professeur Honoraire	M. BOUTAULT Franck
Professeur Honoraire Associé	M. BROS Bernard
Professeur Honoraire	M. BUGAT Roland
Professeur Honoraire	M. CAHUZAC Jean-Philippe
Professeur Honoraire	M. CARATERO Claude
Professeur Honoraire	M. CARLES Pierre
Professeur Honoraire	M. CARON Philippe
Professeur Honoraire	M. CARRIERE Jean-Paul
Professeur Honoraire	M. CARTON Michel
Professeur Honoraire	M. CATHALA Bernard
Professeur Honoraire	M. CHABANON Gérard
Professeur Honoraire	M. CHAMONTIN Bernard
Professeur Honoraire	M. CHAP Hugues
Professeur Honoraire	M. CHAVOIN Jean-Pierre
Professeur Honoraire	M. CLANET Michel
Professeur Honoraire	M. CONTE Jean
Professeur Honoraire	M. COSTAGLIOLA Michel
Professeur Honoraire	M. COTONAT Jean
Professeur Honoraire	M. DABERNAT Henri
Professeur Honoraire	M. DAHAN Marcel
Professeur Honoraire	M. DALOUS Antoine
Professeur Honoraire	M. DALY-SCHVEITZER Nicolas
Professeur Honoraire	M. DAVID Jean-Frédéric
Professeur Honoraire	M. DELSOL Georges
Professeur Honoraire	Mme DELISLE Marie-Bernadette
Professeur Honoraire	Mme DIDIER Jacqueline
Professeur Honoraire	M. DUCOS Jean
Professeur Honoraire	M. DUFFAUT Michel
Professeur Honoraire	M. DUPRE M.
Professeur Honoraire	M. DURAND Dominique
Professeur Honoraire associé	M. DUTAU Guy
Professeur Honoraire	M. ESCHAPASSE Henri
Professeur Honoraire	M. ESCOURROU Jean
Professeur Honoraire	M. ESQUERRE J.P.
Professeur Honoraire	M. FABIÉ Michel
Professeur Honoraire	M. FABRE Jean
Professeur Honoraire	M. FOURNIAL Gérard
Professeur Honoraire	M. FOURNIE Bernard
Professeur Honoraire	M. FOURTANIER Gilles
Professeur Honoraire	M. FRAYSSE Bernard
Professeur Honoraire	M. FREXINOS Jacques
Professeur Honoraire	Mme GENESTAL Michèle
Professeur Honoraire	M. GERAUD Gilles
Professeur Honoraire	M. GHISOLFI Jacques
Professeur Honoraire	M. GLOCK Yves
Professeur Honoraire	M. GOUZI Jean-Louis
Professeur Honoraire	M. GRAND Alain
Professeur Honoraire	M. GUIRAUD CHAUMEIL Bernard
Professeur Honoraire	M. HOFF Jean
Professeur Honoraire	M. JOFFRE Francis
Professeur Honoraire	M. LAGARRIGUE Jacques
Professeur Honoraire	M. LANG Thierry
Professeur Honoraire	Mme LARENG Marie-Blanche
Professeur Honoraire	M. LAURENT Guy
Professeur Honoraire	M. LAZORTHES Franck
Professeur Honoraire	M. LAZORTHES Yves
Professeur Honoraire	M. LEOPHONTE Paul
Professeur Honoraire	M. MAGNAVAL Jean-François
Professeur Honoraire	M. MALECAZE François
Professeur Honoraire	M. MANELFE Claude
Professeur Honoraire	M. MANSAT Michel
Professeur Honoraire	M. MARCHOU Bruno
Professeur Honoraire	M. MASSIP Patrice
Professeur Honoraire	Mme MARTY Nicole
Professeur Honoraire	M. MAZIERES Bernard
Professeur Honoraire	M. MONROZIES Xavier
Professeur Honoraire	M. MOSCOVICI Jacques
Professeur Honoraire	M. MURAT
Professeur Honoraire associé	M. NICODEME Robert
Professeur Honoraire	M. OLIVES Jean-Pierre
Professeur Honoraire	M. PARINAUD Jean
Professeur Honoraire	M. PASCAL Jean-Pierre
Professeur Honoraire	M. PERRET Bertrand
Professeur Honoraire	M. PESSEY Jean-Jacques
Professeur Honoraire	M. PLANTE Pierre
Professeur Honoraire	M. PONTONNIER Georges
Professeur Honoraire	M. POURRAT Jacques
Professeur Honoraire	M. PRADERE Bernard
Professeur Honoraire	M. PRIS Jacques
Professeur Honoraire	Mme PUEL Jacqueline
Professeur Honoraire	M. PUEL Pierre
Professeur Honoraire	M. PUJOL Michel
Professeur Honoraire	M. QUERLEU Denis
Professeur Honoraire	M. RAILHAC Jean-Jacques
Professeur Honoraire	M. REGIS Henri
Professeur Honoraire	M. REGNIER Claude
Professeur Honoraire	M. REME Jean-Michel
Professeur Honoraire	M. RISCHMANN Pascal
Professeur Honoraire	M. RIVIERE Daniel
Professeur Honoraire	M. ROCHE Henri
Professeur Honoraire	M. ROCHICCIOLI Pierre
Professeur Honoraire	M. ROLLAND Michel
Professeur Honoraire	M. ROQUES-LATRILLE Christian
Professeur Honoraire	M. RUMEAU Jean-Louis
Professeur Honoraire	M. SALVADOR Michel
Professeur Honoraire	M. SALVAYRE Robert
Professeur Honoraire	M. SARRAMON Jean-Pierre
Professeur Honoraire	M. SERRE Guy
Professeur Honoraire	M. SIMON Jacques
Professeur Honoraire	M. SUC Jean-Michel
Professeur Honoraire	M. THOUVENOT Jean-Paul
Professeur Honoraire	M. TREMOULET Michel
Professeur Honoraire	M. VALDIGUIE Pierre
Professeur Honoraire	M. VAYSSE Philippe
Professeur Honoraire	M. VINEL Jean-Pierre
Professeur Honoraire	M. VIRENQUE Christian
Professeur Honoraire	M. VOIGT Jean-Jacques

Professeurs Emérites

Professeur ARLET Philippe
Professeur BOUTAULT Franck
Professeur CARON Philippe
Professeur CHAMONTIN Bernard
Professeur CHAP Hugues
Professeur GRAND Alain
Professeur LAGARRIGUE Jacques
Professeur LAURENT Guy
Professeur LAZORTHES Yves
Professeur MAGNAVAL Jean-François
Professeur MARCHOU Bruno
Professeur PERRET Bertrand
Professeur RISCHMANN Pascal
Professeur RIVIERE Daniel
Professeur ROUGE Daniel

FACULTE DE SANTE
Département Médecine Maieutique et Paramédicaux

P.U. - P.H.
Classe Exceptionnelle et 1ère classe

M. ACAR Philippe	Pédiatrie
M. ACCADBLED Franck (C.E)	Chirurgie Infantile
M. ALRIC Laurent (C.E)	Médecine Interne
M. AMAR Jacques	Thérapeutique
Mme ANDRIEU Sandrine	Epidémiologie, Santé publique
M. ARBUS Christophe	Psychiatrie
M. ARNAL Jean-François (C.E)	Physiologie
M. ATTAL Michel (C.E)	Hématologie
M. AVET-LOISEAU Hervé	Hématologie, transfusion
M. BERRY Antoine	Parasitologie
Mme BERRY Isabelle (C.E)	Biophysique
M. BIRMES Philippe	Psychiatrie
M. BONNEVILLE Fabrice	Radiologie
M. BOSSAVY Jean-Pierre (C.E)	Chirurgie Vasculaire
M. BRASSAT David	Neurologie
M. BROUCHET Laurent	Chirurgie thoracique et cardio-vascul
M. BROUSSET Pierre (C.E)	Anatomie pathologique
M. BUJAN Louis (C. E)	Urologie-Andrologie
Mme BURA-RIVIERE Alessandra (C.E)	Médecine Vasculaire
M. BUREAU Christophe	Hépato-Gastro-Entérologie
M. BUSCAIL Louis (C.E)	Hépato-Gastro-Entérologie
M. CALVAS Patrick (C.E)	Génétique
M. CANTAGREL Alain (C.E)	Rhumatologie
M. CARRERE Nicolas	Chirurgie Générale
M. CARRIE Didier (C.E)	Cardiologie
M. CHAIX Yves	Pédiatrie
Mme CHARPENTIER Sandrine	Médecine d'urgence
M. CHAUFOUR Xavier	Chirurgie Vasculaire
M. CHAUVEAU Dominique	Néphrologie
M. CHAYNES Patrick	Anatomie
M. CHIRON Philippe (C.E)	Chir. Orthopédique et Traumatologie
M. CHOLLET François (C.E)	Neurologie
M. CONSTANTIN Arnaud	Rhumatologie
M. COURBON Frédéric	Biophysique
Mme COURTADE SAIDI Monique (C.E)	Histologie Embryologie
M. DAMBRIN Camille	Chir. Thoracique et Cardiovasculaire
M. DE BOISSEZON Xavier	Médecine Physique et Réadapt Fonct.
M. DEGUINE Olivier (C.E)	Oto-rhino-laryngologie
M. DELABESSE Eric	Hématologie
M. DELOBEL Pierre	Maladies Infectieuses
M. DELORD Jean-Pierre (C.E)	Cancérologie
M. DIDIER Alain (C.E)	Pneumologie
M. DUCOMMUN Bernard	Cancérologie
Mme DULY-BOUHANICK Béatrice (C.E)	Thérapeutique
M. ELBAZ Meyer	Cardiologie
M. FERRIERES Jean (C.E)	Epidémiologie, Santé Publique
M. FOURCADE Olivier	Anesthésiologie
M. FOURNIÉ Pierre	Ophtalmologie
M. GALINIER Michel (C.E)	Cardiologie
M. GAME Xavier	Urologie
Mme GARDETTE Virginie	Epidémiologie, Santé publique
M. GEERAERTS Thomas	Anesthésiologie et réanimation
Mme GOMEZ-BROUCHET Anne-Muriel	Anatomie Pathologique
M. GOURDY Pierre (C.E)	Endocrinologie
M. GROLLEAU RAOUX Jean-Louis (C.E)	Chirurgie plastique
Mme GUIMBAUD Rosine	Cancérologie
Mme HANAIRE Hélène (C.E)	Endocrinologie
M. HUYGHE Eric	Urologie
M. IZOPET Jacques (C.E)	Bactériologie-Virologie
M. KAMAR Nassim (C.E)	Néphrologie

P.U. Médecine générale

M. OUSTRIC Stéphane (C.E)

Mme LAMANT Laurence (C.E)	Anatomie Pathologique
M. LANGIN Dominique (C.E)	Nutrition
Mme LAPRIE Anne	Radiothérapie
M. LARRUE Vincent	Neurologie
M. LAUQUE Dominique (C.E)	Médecine d'Urgence
M. LAUWERS Frédéric	Chirurgie maxillo-faciale
M. LEOBON Bertrand	Chirurgie Thoracique et Cardio-vasculaire
M. LEVADE Thierry (C.E)	Biochimie
M. LIBLAU Roland (C.E)	Immunologie
M. MALAVAUD Bernard	Urologie
M. MANSAT Pierre	Chirurgie Orthopédique
M. MARQUE Philippe (C.E)	Médecine Physique et Réadaptation
M. MAS Emmanuel	Pédiatrie
M. MAURY Jean-Philippe (C.E)	Cardiologie
Mme MAZEREEUW Juliette	Dermatologie
M. MAZIERES Julien (C.E)	Pneumologie
M. MINVILLE Vincent	Anesthésiologie Réanimation
M. MOLINIER Laurent (C.E)	Epidémiologie, Santé Publique
M. MONTASTRUC Jean-Louis (C.E)	Pharmacologie
Mme MOYAL Elisabeth (C.E)	Cancérologie
M. MUSCARI Fabrice	Chirurgie Digestive
Mme NOURHASHEMI Fatemeh (C.E)	Gériatrie
M. OLIVOT Jean-Marc	Neurologie
M. OSWALD Eric (C.E)	Bactériologie-Virologie
M. PARIENTE Jérémie	Neurologie
M. PAUL Carle (C.E)	Dermatologie
M. PAYOUX Pierre (C.E)	Biophysique
M. PAYRASTRE Bernard (C.E)	Hématologie
M. PERON Jean-Marie (C.E)	Hépato-Gastro-Entérologie
M. RASCOL Olivier (C.E)	Pharmacologie
Mme RAUZY Odile	Médecine Interne
M. RAYNAUD Jean-Philippe (C.E)	Psychiatrie Infantile
M. RECHER Christian(C.E)	Hématologie
M. RITZ Patrick (C.E)	Nutrition
M. ROLLAND Yves (C.E)	Gériatrie
M. RONCALLI Jérôme	Cardiologie
M. ROUGE Daniel (C.E)	Médecine Légale
M. ROUSSEAU Hervé (C.E)	Radiologie
M. ROUX Franck-Emmanuel	Neurochirurgie
M. SAILLER Laurent (C.E)	Médecine Interne
M. SALES DE GAUZY Jérôme (C.E)	Chirurgie Infantile
M. SALLES Jean-Pierre (C.E)	Pédiatrie
M. SANS Nicolas	Radiologie
M. SCHMITT Laurent (C.E)	Psychiatrie
Mme SELVES Janick (C.E)	Anatomie et cytologie pathologiques
M. SENARD Jean-Michel (C.E)	Pharmacologie
M. SERRANO Elie (C.E)	Oto-rhino-laryngologie
M. SIZUN Jacques (C.E)	Pédiatrie
M. SOL Jean-Christophe	Neurochirurgie
Mme SOTO-MARTIN Maria-Eugénia	Gériatrie et biologie du vieillissement
M. SOULAT Jean-Marc	Médecine du Travail
M. SOULIE Michel (C.E)	Urologie
M. SUC Bertrand	Chirurgie Digestive
Mme TAUBER Marie-Thérèse (C.E)	Pédiatrie
M. TELMON Norbert (C.E)	Médecine Légale
Mme TREMOLLIERES Florence	Biologie du développement
Mme URO-COSTE Emmanuelle (C.E)	Anatomie Pathologique
M. VAYSSIERE Christophe (C.E)	Gynécologie Obstétrique
M. VELLAS Bruno (C.E)	Gériatrie
M. VERGEZ Sébastien	Oto-rhino-laryngologie

FACULTE DE SANTE
Département Médecine Maieutique et Paramédicaux

P.U. - P.H.
2ème classe

M. ABBO Olivier	Chirurgie infantile
M. AUSSEIL Jérôme	Biochimie et biologie moléculaire
Mme BONGARD Vanina	Epidémiologie, Santé publique
M. BONNEVIALLE Nicolas	Chirurgie orthopédique et traumatologique
M. BOUNES Vincent	Médecine d'urgence
Mme BOURNET Barbara	Gastro-entérologie
Mme CASPER Charlotte	Pédiatrie
M. CAVAIGNAC Etienne	Chirurgie orthopédique et traumatologie
M. CHAPUT Benoit	Chirurgie plastique
M. COGNARD Christophe	Radiologie
Mme CORRE Jill	Hématologie
Mme DALENC Florence	Cancérologie
M. DE BONNECAZE Guillaume	Anatomie
M. DECRAMER Stéphane	Pédiatrie
M. EDOUARD Thomas	Pédiatrie
M. FAGUER Stanislas	Néphrologie
Mme FARUCH BILFELD Marie	Radiologie et imagerie médicale
M. FRANCHITTO Nicolas	Addictologie
M. GARRIDO-STÖWHAS Ignacio	Chirurgie Plastique
M. GUIBERT Nicolas	Pneumologie
M. GUILLEMINAULT Laurent	Pneumologie
M. HERIN Fabrice	Médecine et santé au travail
M. LAIREZ Olivier	Biophysique et médecine nucléaire
M. LAROCHE Michel	Rhumatologie
Mme LAURENT Camille	Anatomie Pathologique
M. LE CAIGNEC Cédric	Génétique
M. LEANDRI Roger	Biologie du dével. et de la reproduction
M. LOPEZ Raphael	Anatomie
M. MARCHEIX Bertrand	Chirurgie thoracique et cardiovasculaire
M. MARTIN-BLONDEL Guillaume	Maladies infectieuses, maladies tropicales
Mme MARTINEZ Alejandra	Gynécologie
M. MARX Mathieu	Oto-rhino-laryngologie
M. MEYER Nicolas	Dermatologie
M. PAGES Jean-Christophe	Biologie cellulaire
Mme PASQUET Marlène	Pédiatrie
M. PORTIER Guillaume	Chirurgie Digestive
M. PUGNET Grégory	Médecine interne
M. REINA Nicolas	Chirurgie orthopédique et traumatologique
M. RENAUDINEAU Yves	Immunologie
Mme RUYSSEN-WITRAND Adeline	Rhumatologie
Mme SAVAGNER Frédérique	Biochimie et biologie moléculaire
M. SAVALL Frédéric	Médecine légale
M. SILVA SIFONTES Stein	Réanimation
M. SOLER Vincent	Ophtalmologie
Mme SOMMET Agnès	Pharmacologie
M. TACK Ivan	Physiologie
Mme VAYSSE Charlotte	Cancérologie
Mme VEZZOSI Delphine	Endocrinologie
M. YRONDI Antoine	Psychiatrie
M. YSEBAERT Loic	Hématologie

P.U. Médecine générale
M. MESTHÉ Pierre
Mme ROUGE-BUGAT Marie-Eve

Professeurs Associés

Professeur Associé de Médecine Générale
M. ABITTEBOUL Yves
Mme BOURGEOIS Odile
M. BOYER Pierre
M. CHICOULAA Bruno
Mme IRI-DELAHAYE Motoko
M. PIPONNIER David
M. POUTRAIN Jean-Christophe
M. STILLMUNKES André

Professeur Associé de Bactériologie-Hygiène
Mme MALAVAUD Sandra

FACULTE DE SANTE
Département Médecine Maieutique et Paramédicaux

MCU - PH

Mme ABRAVANEL Florence	Bactériologie Virologie Hygiène
M. APOIL Pol Andre	Immunologie
Mme ARNAUD Catherine	Epidémiologie
Mme AUSSEIL-TRUDEL Stéphanie	Biochimie
Mme BASSET Céline	Cytologie et histologie
Mme BELLIERES-FABRE Julie	Néphrologie
Mme BERTOLI Sarah	Hématologie, transfusion
M. BIETH Eric	Génétique
Mme BREHIN Camille	Pneumologie
M. BUSCAIL Etienne	Chirurgie viscérale et digestive
Mme CAMARE Caroline	Biochimie et biologie moléculaire
M. CAMBUS Jean-Pierre	Hématologie
Mme CANTERO Anne-Valérie	Biochimie
Mme CARFAGNA Luana	Pédiatrie
Mme CASPAR BAUGUIL Sylvie	Nutrition
Mme CASSAGNE Myriam	Ophtalmologie
Mme CASSAING Sophie	Parasitologie
Mme CASSOL Emmanuelle	Biophysique
Mme CHANTALAT Elodie	Anatomie
M. CHASSAING Nicolas	Génétique
M. CLAVEL Cyril	Biologie Cellulaire
Mme COLOMBAT Magali	Anatomie et cytologie pathologiques
M. CONGY Nicolas	Immunologie
Mme COURBON Christine	Pharmacologie
M. CUROT Jonathan	Neurologie
Mme DAMASE Christine	Pharmacologie
Mme DE GLISEZENSKY Isabelle	Physiologie
M. DEDOUIT Fabrice	Médecine Légale
M. DEGBOE Yannick	Rhumatologie
M. DELMAS Clément	Cardiologie
M. DELPLA Pierre-André	Médecine Légale
M. DESPAS Fabien	Pharmacologie
M. DUBOIS Damien	Bactériologie Virologie Hygiène
Mme ESQUIROL Yolande	Médecine du travail
Mme EVRARD Solène	Histologie, embryologie et cytologie
Mme FILLAUX Judith	Parasitologie
Mme FLOCH Pauline	Bactériologie-Virologie
Mme GALINIER Anne	Nutrition
Mme GALLINI Adeline	Epidémiologie
M. GANTET Pierre	Biophysique
M. GASQ David	Physiologie
M. GATIMEL Nicolas	Médecine de la reproduction
Mme GENNERO Isabelle	Biochimie
Mme GENOUX Annelise	Biochimie et biologie moléculaire
Mme GRARE Marion	Bactériologie Virologie Hygiène
M. GUERBY Paul	Gynécologie-Obstétrique
Mme GUILBEAU-FRUGIER Céline	Anatomie Pathologique
Mme GUYONNET Sophie	Nutrition
M. HAMDI Safouane	Biochimie
Mme HITZEL Anne	Biophysique
Mme INGUENEAU Cécile	Biochimie
M. IRIART Xavier	Parasitologie et mycologie
Mme JONCA Nathalie	Biologie cellulaire
M. KIRZIN Sylvain	Chirurgie générale
Mme LAPEYRE-MESTRE Maryse	Pharmacologie
M. LEPAGE Benoit	Biostatistiques et Informatique médicale
M. LHERMUSIER Thibault	Cardiologie
M. LHOMME Sébastien	Bactériologie-virologie
Mme MASSIP Clémence	Bactériologie-virologie
Mme MAUPAS SCHWALM Françoise	Biochimie
Mme MONTASTIER Emilie	Nutrition
M. MONTASTRUC François	Pharmacologie
Mme MOREAU Jessika	Biologie du dév. Et de la reproduction
Mme MOREAU Marion	Physiologie
M. MOULIS Guillaume	Médecine interne
Mme NASR Nathalie	Neurologie
Mme NOGUEIRA M.L.	Biologie Cellulaire
Mme PERROT Aurore	Hématologie
M. PILLARD Fabien	Physiologie
Mme PLAISANCIE Julie	Génétique
Mme PUISSANT Bénédicte	Immunologie
Mme QUELVEN Isabelle	Biophysique et médecine nucléaire
Mme RAYMOND Stéphanie	Bactériologie Virologie Hygiène
M. REVET Alexis	Pédo-psychiatrie
M. RIMAILHO Jacques	Anatomie et Chirurgie Générale
Mme SABOURDY Frédérique	Biochimie
Mme SAUNE Karine	Bactériologie Virologie
Mme SIEGFRIED Aurore	Anatomie et cytologie pathologiques
M. TAFANI Jean-André	Biophysique
M. TREINER Emmanuel	Immunologie
Mme VALLET Marion	Physiologie
M. VERGEZ François	Hématologie
Mme VIJA Lavinia	Biophysique et médecine nucléaire

M.C.U. Médecine générale

M. BISMUTH Michel
M. BRILLAC Thierry
Mme DUPOUY Julie
M. ESCOURROU Emile

Maîtres de Conférence Associés

M.C.A. Médecine Générale

M. BIREBENT Jordan
Mme BOUSSIER Nathalie
Mme FREYENS Anne
Mme LATROUS Leila
Mme PUECH Marielle

REMERCIEMENTS AU JURY

A Monsieur le Professeur Hervé ROUSSEAU, Président du Jury
Professeur des Universités – Praticien Hospitalier
Chef du Service de Radiologie de Rangueil
Je vous remercie de me faire l'honneur de présider cette soutenance.
Je vous remercie également pour la bienveillance et l'implication que vous avez portées à mon parcours de formation durant cet internat.
C'est en grande partie au sein de votre service que j'ai découvert et que je continue à apprendre la radiologie telle que je souhaite l'exercer.
Soyez assuré de ma reconnaissance et de mon respect.

A Madame le Professeur Fatima Zohra MOKRANE, Directrice de Thèse
Professeur des Universités – Praticien Hospitalier
Service de Radiologie de Rangueil
Merci pour ta passion de la pédagogie, et pour m'avoir proposé ce travail. Merci également pour ta confiance, tes encouragements durant ces années de formation. Quel plaisir d'apprendre et de progresser à tes côtés !

A Madame le Docteur Céline MOULY, Assesseur
Service d'Endocrinologie et maladies métaboliques, Hôpital Larrey
Je vous remercie pour votre disponibilité, et votre aide dans la relecture de ce travail.
Je vous remercie également d'avoir accepté de participer à ce jury.
Soyez assurée de ma gratitude et de mon respect.

A Monsieur le Docteur Matthieu THOULOUZAN, Assesseur
Service de Chirurgie Urologique, Hôpital Rangueil
Je vous remercie d'avoir accepté de critiquer ce travail, de nous y faire bénéficier de votre vision de chirurgien, et de vous être rendu disponible pour participer à ce jury.
Soyez assuré de ma gratitude et de mon respect.

A Monsieur le Docteur Lawrence DIERICKX, Assesseur
Service de Médecine nucléaire et oncologie nucléaire, Institut Universitaire du Cancer Toulouse
Je vous remercie pour votre disponibilité.
Je vous remercie également d'avoir accepté de participer à ce jury pour critiquer ce travail et y apporter de futures perspectives.
Soyez également assuré de ma gratitude et de mon respect.

A Monsieur le Docteur Laurent DERCLE, Membre Invité
MD, PhD Nuclear Medicine, New York-Presbyterian Hospital/Columbia University Irving Medical Center Department of Radiology
Je vous remercie pour vos conseils qui m'ont aidé à initier ce travail. Merci également d'avoir accepté de participer à ce jury pour critiquer ce travail
Je vous prie de recevoir ma gratitude et mon respect.

REMERCIEMENTS A MES MAITRES, CHEFS, ASSISTANTS

Aux radiologues des différents services où j'ai été formé, pour leur disponibilité, leurs conseils, leur pédagogie.

Au sein du CHU de Rangueil :
Merci énormément pour m'avoir transmis votre passion, en journée comme en garde. C'est un plaisir chaque jour de travailler avec vous.
Charline, pour ta bienveillance et disponibilité permanente; **Alexandre**, pour ta patience, ta disponibilité ; **Philippe**, pour l'investissement pédagogique dont le service bénéficie tous les lundi soirs ; **Séverine**, pour tes enseignements et ta bienveillance. **Samia**, pour ta rigueur et tes conseils durant ce stage d'imagerie cardiaque; **Marie Agnès**, pour tes enseignements en imagerie cardiaque ; **Pierre**, pour ces vacations de scanner et sessions de bloc formatrices, dans la bonne humeur ; **Paul**, pour tes connaissances et ta bienveillance dans l'encadrement des internes ; **Micha**, pour tes conseils au bloc ; **Chloé**, pour ta gentillesse ; **Adrien**, pour tous ces bons de biopsies « OK Vava NQNQ » ; **Aris, Nico, Baptiste, François, Ephraïm,** pour votre encadrement durant ces années d'internat.

Au sein du CHU de Purpan :
Aux équipes des **Professeurs Marie FARUCH, Fabrice BONNEVILLE, Nicolas SANS, Christophe COGNARD**, pour les enseignements que j'ai pu recevoir dans vos services.
Merci aux PH, chefs et assistants qui y ont pris le temps de participer à ma formation de futur radiologue : Gilles, Margot, Sofia, Annick, Jean, Philippe, Raluca, Maxence, Céline, Rafy, Romain, Florent, Hubert, Frank, Hélène, Louise, Léa, Samantha, Sarah, Sophie.

Merci également aux radiologues des CH où je suis passé pour leur accueil et leur disponibilité, notamment les Docteurs DUBOIS, DULAURANS, LIVIDEANU, RENGEL, SILVESTER.

Au personnel paramédical, et aux patients, qui depuis maintenant une quinzaine d'année m'aident peu à peu à devenir un meilleur médecin.

Au jury de la commission de passerelle de Toulouse Bordeaux, pour m'avoir donné il y a maintenant neuf ans la chance d'exercer mon droit au remord pour revenir en médecine.

REMERCIEMENTS PERSONNELS

A mes grands-parents, Suzanne, Bernard, Jean, Madeleine. Pour ces moments heureux et simples au bord de la mer, durant mon enfance.

A mes parents, merci de m'avoir accompagné, soutenu, au long de ces longues années d'étude. Votre confiance et vos encouragements ont été ma principale source de motivation pour reprendre les études médicales et y donner le meilleur de moi-même. Je me lève tous les matins pour faire un métier que j'aime, et c'est grâce à vous.
A mes deux frangins d'exception, **Erwann** l'imageur pêcheur, **Brieuc** l'ingénieur rêveur. Pour tous ces bons moments ensemble, passés et à venir.
A Anaïs, Paul et Baptiste, qui amenez chaque jour un peu plus de bonheur dans cette famille.
A mes oncles, tantes, cousins, cousines, pour tous ces souvenirs de bons moments passés ensemble.

A Noé, toi qui m'as en grande partie convaincu de choisir l'imagerie médicale au concours l'ECN. Merci pour tes conseils et encouragements durant ce cursus. Merci pour ton soutien, et ton amitié constante, durant ces années, même durant les moments difficiles.
A Nat et Mat, et votre petite Eva, pour votre soutien, votre bonne humeur et votre bienveillance également durant ces années.
A Lulu, notre télé-radiologue en slip, ami sincère et intransigeant.
A Sylvain, Amandine, sans oublier votre petite Alice, pour vos preuves d'amitiés constantes.

Aux plongeurs associatifs du club ADLM, du monde de la plongée souterraine, pour cette passion et ces compétences que vous m'avez transmises. A **François**, mon binôme de choc pour nos sorties plongées, en mer et sous terre. A **Sophie, Cédric.**

Aux copains maintenant un peu partout en France : Clem et Djo, Florian, Regis, Jeff, Dest, Jonathan, Virgule, Marsouin, Nico, Matt, Jeb, Jerem, Pascal, Jean mat, Helene, Kepa, Loik, Marco.
Fred, Guillaume, Aymeric, Polo, Thomas, Bastien, pour votre amour des bonnes tablées.
Amandine N., continue à faire d'aussi belles photos !

A mes anciens coexternes, pour tous ces souvenirs et repas durant les durs moments de l'externat. Quel plaisir de se retrouver régulièrement ! **Cam et Estela, Loulou, Stouph, Pierrot, Camzouz**. A **Raphaël et Gaetan**, pour ces longues sous-colles qu'on s'infligeait pour donner le meilleur de nous-même.

A la team Carcassoss' pour tous ces supers moments passés ! **Léa et Laetitia, Ophélie, Mélanie L et Mélanie L, Coralya, Léonie, Laurent, Arthur**, **Antoine, Gilette, Maud**.
A la team du lobby, pour ces bons moments de rigolade ! **Nico**, **LC, Albert, Gwen, Chris, Tom.**

A mes co-internes, même si cet internat passe trop vite et qu'il est difficile de tous bien se connaître…
Merci particulièrement à celles et ceux qui m'ont encadré lors de mes jeunes semestres et pris le temps de participer à ma formation : **Rayan, Emmanuel, Constance, Sarah**.
Merci également à celles et ceux qui m'ont accompagné durant ces semestres : **Hamza H, Hamza L, Nithida, Totor, Mathieu S, Julien C, Julien D, Joe, Sabine, Justine, Imen, Alexia, Céline, Arthur, Elorie, Guilhem, Jeff, Louis, Sylvain, Rokia, Thomas, Thibaut, Marina, Tam, Julie K, Julie A, Johan, Philippe, Antoine, Marie-Claire**.

A mes amis de lycée, **Jean Philippe, Antoine, Mickael**, toujours présents malgré les années.
A **Valentine**, pour la gastronomie, l'œnologie, et cette drôle de passion pour l'ornithologie.

THE ROLE OF IMAGE-GUIDED PRECISION MEDICINE IN THE DIAGNOSIS AND TREATMENT OF PHEOCHROMOCYTOMAS AND PARAGANGLIOMAS IN THE ERA OF IMAGING BIOMARKERS AND ARTIFICIAL INTELLIGENCE

Abstract:

Metastatic pheochromocytomas and paragangliomas are rare neural-crest-derived tumors with variable prognosis. In an era of tailored treatment strategies, medical imaging plays a crucial role in the surgeries, image-guided procedures, chemotherapies, immunotherapies and radionuclide therapies involved in the diagnosis and treatment of these tumors. Medical imaging helps to confirm the diagnosis, guide surgical resection, assess metastatic staging, and select patients for specific therapies. In this step-by-step review, we perform a comprehensive analysis of recent imaging modalities developed for pheochromocytomas and paragangliomas by covering their content and terminology as well as discussing the future implications of artificial intelligence.
Key words:
Pheochromocytoma, Paraganglioma, Imaging, Artificial intelligence, Somatostatin receptors

KEY POINTS

- This review emphasizes the growing importance of anatomical and molecular medical imaging in the diagnosis, treatment and response assessment of patients with pheochromocytomas and paragangliomas.
- Medical imaging enables personalized management and improved outcomes when employed in tailored strategies.
- Medical imaging provides a non-invasive and comprehensive assessment of a tumor's spatial and temporal heterogeneity.
- The diagnostic accuracy of medical imaging varies with tumor type and genetic background, which is crucial for guiding curative surgery or palliative cytoreduction.
- Interventional radiology is a constantly evolving field (e.g., thermal ablations, intra-arterial embolizations, and selective internal radiotherapy).
- Response assessments should be tailored to the type of systemic treatments, such as chemotherapies, targeted therapies, immunotherapies and internal radiotherapies.

ABBREVIATIONS

ADC apparent diffusion coefficient
AJCC American Joint Committee on Cancer
ASII adrenal signal intensity index
CEUS contrast enhanced ultrasound examination
CE- MRA constrast-enhanced MR angiography
CT computed tomography
CgA Plasma chromogranin A
CSI chemical shift imaging
DCE dynamic contrast enhanced
DOPA dihydroxyphenylalanine
DOTATOC $DOTA^{0}$-Phe^{1}-Tyr^{3} octreotide
DWI diffusion-weighted imaging
ECL enterochromaffin-like
ENETs European Neuroendocrine Tumor Society
^{18}F-FDG ^{18}Fluoro-Fluorodeoxyglucose
^{68}Ga ^{68}Gallium
GEP gastroenteropancreatic
GLP-1 Glucagon-like peptide 1
HaN PGL head and neck paraganglioma
IACIG *intra-arterial injection of calcium*
Ifα Interferon α
IOUS intra operative ultrasound examination
^{177}Lu ^{177}Lutetium
M/NM metanephrine/normetanephrine
MRI magnetic resonance imaging
NANETS North American Neuroendocrine Tumor Society
NET neuroendocrine tumors
NF1 neurofibromatosis type 1
OS overall survival
PCC pheochromocytoma
PD-L1 Programmed death-ligand 1
PET positron emission tomography
PERCIST PET Response Criteria in Solid Tumors
PFS progression-free survival
pNET pancreatic neuroendocrine tumor
PPGLs pheochromocytomas and paragangliomas, if metastatic : **MPPGLS**
PR partial response
PRRT peptide receptor radionuclide therapy
RECIST Response Evaluation Criteria in Solid Tumors
SD stable disease
SDHx Succinate DeHydrogenase genetic alterations
SSA somatostatin analogs
SSTR somatostatin receptor
SSTR-PET Somatostatin receptor PET
SSTR scintigraphy Somatostatin receptor scintigraphy
SUV standard uptake value
T1-w or **T2-w** : T1-weighted or T2-weighted (MRI sequence)
TACE transarterial chemo-embolization
TAE transarterial embolization

US ultra sound examination
WHO World Health Organization
^{90}Y ^{90}Yttrium

TABLE DES MATIERES

Introduction

Pheochromocytomas (PCCs) and paragangliomas (PGLs) are both (PPGLs) rare neural-crest-derived tumors. Thanks to the latest advances in medical imaging, diagnoses of PPGLs have increased. For example, 4% of incidentally discovered adrenal masses are proven to be a pheochromocytoma[1]. Although they share the same histological origin, PCCs and PGLs differ in several aspects, such as functional status, metastatic potential and risk of recurrence. Improvements in imaging biomarkers and artificial intelligence over the past few decades offer tailored diagnostic and treatment strategies based on a tumor's genetic and inherent phenotypic background. This guide provides an innovative image modality-based approach to PPGLs (except head and neck locations) imaging and management through its review of each imaging modality, the specifics of each treatment option and the current imaging reporting systems available to improve follow-up. A special focus on imaging biomarkers and artificial intelligence will also be discussed in this comprehensive review.

I) Epidemiology, genetics and molecular background: how to stratify risk

Embryology. PPGLs arise from adrenal medulla (PCCs) and the extra-adrenal paravertebral sympathetic ganglia (PGLs) of the thorax, abdomen, pelvis. Head and neck paragangliomas (HaN PGLs) arise specifically from the parasympathetic structures at the base of the skull along the glossopharyngeal (CN IX) and vagal (CN X) nerves. The incidence of diagnosed PPGLs is about 0.2-0.8/100,000 patients/year[2] with a reported PCC/PGL ratio of 80%/20%[3]. The prevalence is reported to be 0.2 to 0.6% in adults and 1.7% in children with hypertension[1]. Over the past few decades, the annual age-standardized incidence rates have increased with a higher age at diagnosis alongside significantly smaller PCC tumor sizes. This is mainly due to improvements in clinical practice and targeted screening plasma and urinary free metanephrine/normetanephrine (M/NM), increased use of imaging studies and screening of susceptibility gene related-carriers)[4].

Tumor functional status. PPGLs belong to the neuro-endocrine tumor (NET) group, and are able to produce, store and secrete one or more catecholamines: M/NM and dopamine. This catecholamine-secreting function is mainly observed in sympathetic tissue-derived PCCs and PGLs arising below the head and neck (in 96% and 65% of tumors, respectively),

whereas the majority (97%) of parasympathetic HaN PGLs are non-secreting[5]. The catecholamine excess explains the adverse symptoms that characterize initial presentations of NETs (e.g., hypertension, headaches, sweating and palpitations) as well as their related acute complications (e.g., renal failure, intestinal ischemia, heart attack, angina, pulmonary edema, osteoporosis and pathological fractures[6–9]). Due to their endocrine function, plasma and 24h-urinary M/NM measurements are the recommended biochemical tests for PPGLs, both for screening and follow-up, sometimes completed with 3-methoxytyramine serum evaluation.

Therefore, this screening is critical before any biopsy in case of suspected PPGL, to prevent life-threatening outcomes[10].

However, rare false-negatives (small PCCs and non-secreting PGLs), and medication-induced false-positives (diuretics, b-blockers, tricyclic antidepressants, renal failure, acute stress…) can alter their performance[11]. Another plasma protein of interest, chromogranin A (CgA), is stored and released along with catecholamines. Serum CgA levels are elevated in almost all NETs including PPGLs, suggesting that serum CgA may be an alternative for screening and follow-up in the outpatient setting, even if false-positive exist. Currently serum CgA use is limited to preoperative evaluation of NET patients with otherwise normal M/NM levels and postoperative follow-up in patients with elevated CgA [12,13].

Genetics. PPGLs are part of inherited tumor syndromes in 40% of cases. More than 20 genes have been identified (such as SDHD, VHL, RET, neurofibromatosis type 1 NF1), including inherited cancer susceptibility genes[5,14–19]. Comprehensive molecular research has defined four groups with specific pathways depending on the identified mutated driver and fusion genes : c kinase signaling subtype, pseudohypoxia subtype, Wnt-altered subtype and cortical admixture subtype[20]. Each genetic underlying mutation has a specific risk of metastatic outcome, multifocal disease, and familial history. Genetic testing is an essential component of not only patient management, follow-up and prognostication but also choosing an optimal imaging modality[21]. For instance, metastatic risk is low in PCCs (5-10%), high in PGLs (30-35%), and even higher in Succinate DeHydrogenase genetic alterations group (SDHx) such as SDHB mutations carriers (up to 80% in some series)[22]. SDHB and SDHC mutations have autosomal dominant inheritance, at risk of earlier PPGLs (mean age at diagnosis 35-40 years, lifetime risk 30%), with a less-differentiated phenotype, a higher risk of metastatic disease at diagnosis or during follow-up[8,23–25] and a poorer prognosis[26]. Therefore, early diagnosis of patients and their relatives is critical in improving overall prognosis. Several algorithms

based on immunohistochemical staining procedures and genetic screening are currently being implemented in routine practice guidelines[27–29].

Grade and metastatic status. Despite the latest progress in the understanding of PPGLs, there is still no histological, molecular, or genetic criteria of malignancy. According to the latest WHO classification[30], malignancy in PPGLs is only defined by proven distant metastases in non-chromaffin tissues (mainly bone, lung, lymph nodes and liver), even if histologic patterns were reported to be indicative of malignancy, such as small cell or spindle cell patterns[31,32]. In 2017, the American Joint Committee on Cancer (AJCC) proposed a TNM staging[33] classification with a prognostic value (worse survival in stage IV)[34]. According to this classification, the terms 'malignant' and 'benign' should be abandoned with the intention that all PPGLs are classified as having malignant potential[30,35].

PGL metastases are reported to occur earlier than PCC metastases (median age 36 years vs 46 years), with more synchronous metastatic disease at diagnosis (41% vs 26%)[36]. Radiologists must be aware that the most common metastatic sites are bone (60-70% of metastatic patients), lymph nodes (47%), liver/lung/thorax (38%) and abdomen/pelvis (32%) with PGL metastases mostly spreading to lymph nodes (67%) and PCC metastases mostly spreading to the liver (49-57%)[25,37–39].

Prognosis and prognostic markers. The 5-year survival rate for cases of malignant PPGLs varies from 50% to 80%[24], with a metastatic risk reported to be 4-5 times higher in PGLs than PCCs[36,40]. Beside genetic status discussed earlier[26], some factors are reportedly associated with worse survival: male sex, synchronous metastases, larger tumor size (>5cm), hypersecretion, dopamine secretion phenotype and serum levels of the dopamine metabolite 3-methoxytyramine[25,31,36,40–43]. Ki-67 antigen is a nuclear protein expressed only in proliferating cells with a high prognostic value in NETs[44]. This antigen has an unclear prognostic value in PPGLs[31,43,45–47], even though it was recently reported to be a significant prognostic factor for locally advanced PCCs [48], and to be significantly higher in metastatic PCCs[49], with a cut-off >2-3%.

Several scores are used to better risk stratify patients with PPGLs, based on histological grade (The PASS Pheochromocytoma scaled score, the GAPP Grading of Adrenal Pheochromocytoma and Paraganglioma score[50,51]) or clinical presentation (The ASES score[52]). These scores have high negative predictive values (PASS score, up to 99%[32,42,53]),

but significantly different survival rates, requiring validation from multicenter clinical trials[50].

The majority of histological criteria are applied to post-operative histological analysis. However, imaging modalities can preoperatively shed light on certain poor prognostic factors. For instance, lesions larger than 5cm are at higher risk of malignancy [41,54]. Additionally, since the GAPP score uses histological cellularity as a main prognostic criterion, MRI diffusion sequences may be a useful alternative for assessing cellularity, although this has yet to be proven[55].

II) Anatomical imaging techniques

Recommendations for exploration of an indeterminate adrenal mass[56,57]. Although PCCs may be discovered when working up patients with a catecholamine syndrome and abdominal pain, they can also first present as incidental findings on abdominal imaging[58]. For adrenal incidentalomas, the European Society of Endocrinology recommends performing a clinical exam, biological screening and conventional imaging (non-contrast CT for adults, or abdominal MRI otherwise). Benign features on non-contrast CT imaging include: attenuation value <10 Hounsfield units (HU), size <4cm and homogeneity. If all criteria are met, no further imaging is required. Otherwise, a contrast enhanced CT examination or MRI with chemical shift imaging is necessary.

Additional value of contrast enhanced CT scan (CE-CT scan). CE-CT scan assesses washout characteristics of adrenal masses after enhancement by comparing the attenuation values at specific times and calculating percentages of absolute and relative washouts (**Fig. 1**). An absolute enhancement washout ≥ 60% and relative enhancement washout ≥ 40% are 96-100% specific for adenoma. False positives are rare but have been reported, such as lipid-rich PCC[59] or renal metastases with increased washout[60].

Additional value of MRI with chemical shift imaging (CSI). This technique is an alternative to CE-CT scan, and takes advantage of adenoma cells' high lipid content, which induces variations in the signal intensity (SI) of the adrenal lesion in the MRI in-phase (ip) compared to the out-phase (op). These values are compared to the spleen's to calculate the adrenal lesion to spleen ratio (ASR) and adrenal signal intensity index (ASII).

ASR is either calculated in publications as (SIop adrenal mass / SIop spleen) / (SIip adrenal mass/SIip spleen) to assess remaining signal expected to be inferior to 0.71 for the diagnosis of adenoma[61], or as [(SIop adrenal mass / SIop spleen) / (SIip adrenal mass/SIip spleen)-1] to calculate percentage of signal loss, expected to be inferior to -35.9%[62] (**Fig. 2**).

ASII is an alternative calculated as (SIip adrenal mass - SIop adrenal mass)/(SIipadrenal mass) x 100 (signal remaining). Diagnosis of adenoma is achieved when SII is superior to 16.5% (1.5T)[63].

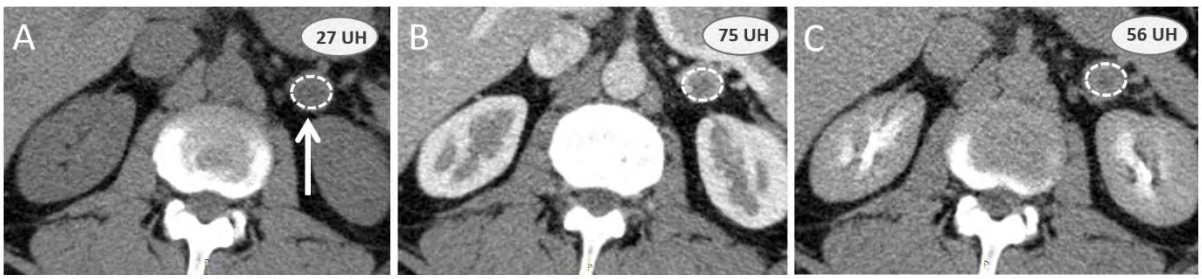

Fig. 1-*Adrenal CE-CT scan washout calculation.*

CT examination in a 54-year-old male patient with non enhanced (A), arterial (B) and 10 minute delayed (C) phases is performed to evaluate an incidental adrenal mass (white arrow). Non-enhanced attenuation value of this adrenal mass is greater than 10 UH (27 UH), which lead to the performance of a CE-CT scan (arterial and 10-minutes delayed phases attenuation respectively of 75 UH and 56 UH). Absolute and relative washouts are respectively of 50% and 32% respectively do not favor benign adrenal adenoma. Surgery is performed, with final diagnosis of sporadic non-secreting PCC.

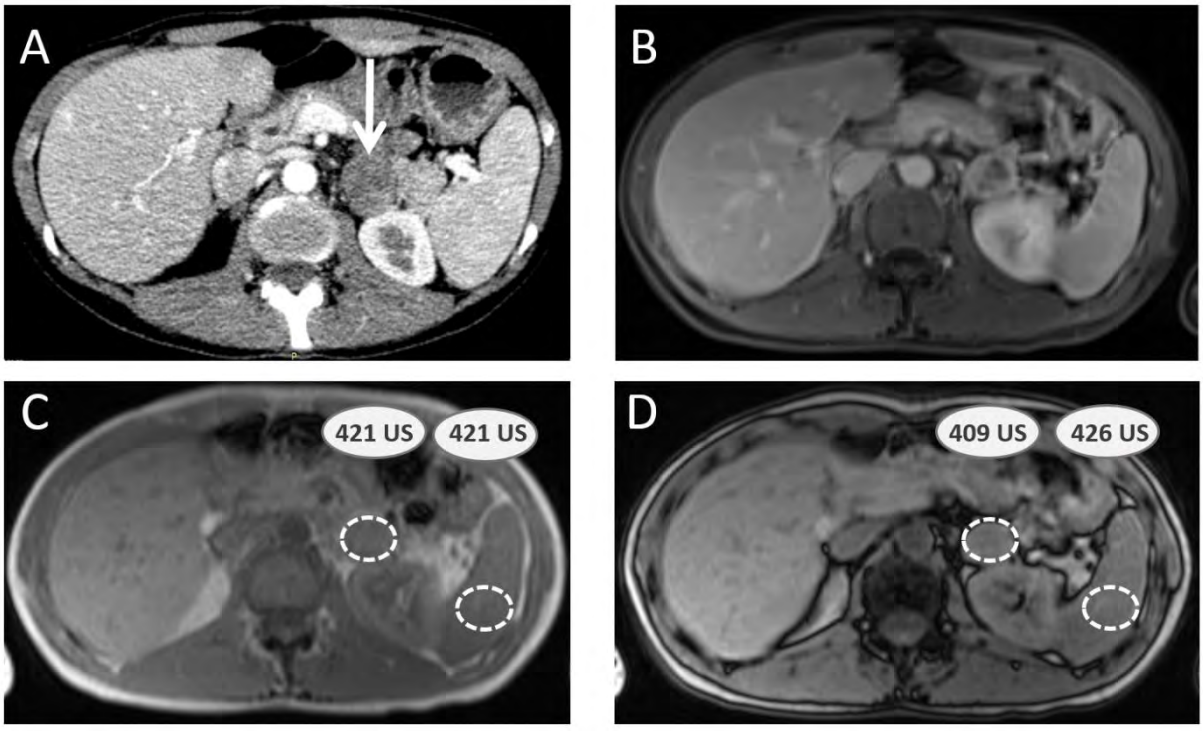

Fig. 2-*Adrenal-to-spleen ratio (ASR) MRI calculation.*

40-year-old female patient with NEM2A syndrom presents with a left adrenal mass (white arrow) on CT scan (A). MRI is performed, including gadolinium-enhanced sequence (B) and chemical shift sequences (C: IN unit signal values in adrenal mass and spleen parenchyma, D: OUT unit signal values in same spots), providing an ASR with remaining signal of 0,96 over benign adenoma cut-off (0,71). Surgery confirmed PCC, with no metastases seven years later.

Morphological characteristics of PPGLs using anatomical imaging. CT and MR examinations provide important information on preoperative localization of a tumor, even if their characterization performances can be limited. PPGLs are reported to have strong enhancement after injection of contrast agent and a slow washout. Around half of PPGLs are reported to be homogeneous and hypointense in T1-weighted (T1-w) and markedly hyperintense in T2-weighted (T2-w) MRI sequences compared to spleen and liver, with possible "salt and pepper " appereance related to flow voids in tumor vessels. The rest of PPGLs are more heterogeneous with mixed areas of high and low signal intensity, which are possibly cystic lesions or swirl-like areas that correspond with hemorrhage or necrosis spots on histopathology. (**Fig. 3**). However, enhancement patterns and other radiological criteria of aggressiveness used in other solid tumors (i.e., ill-defined contours, heterogeneity...) did not have any relationship with potential risk of malignancy [61].

PCCs can take several morphologic presentations, with cystic, haemorragic or heterogeneous components. Contribution of enhancement phases, multiplanar reconstructions and multimodal imaging is crucial. **A** Multimodality imaging with ultrasonographic and CE-CT images of a high-volume mainly-solid left PCC (arrow head) in a 63-year-old female patient suffering adrenergic syndrom (Tako-Tsubo syndrom, drug resistant hypertension). **B** Axial, coronal and sagittal CE-CT scan of a high volume left PCC with necrotic center (arrowhead) in a 32-year-old female patient with NEM2A syndrom (PASS4). **C** Axial and coronal CE-CT scan of a high volume, cystic right PCC (arrowhead) in a 47-year-old male patient without susceptibility genetic background.

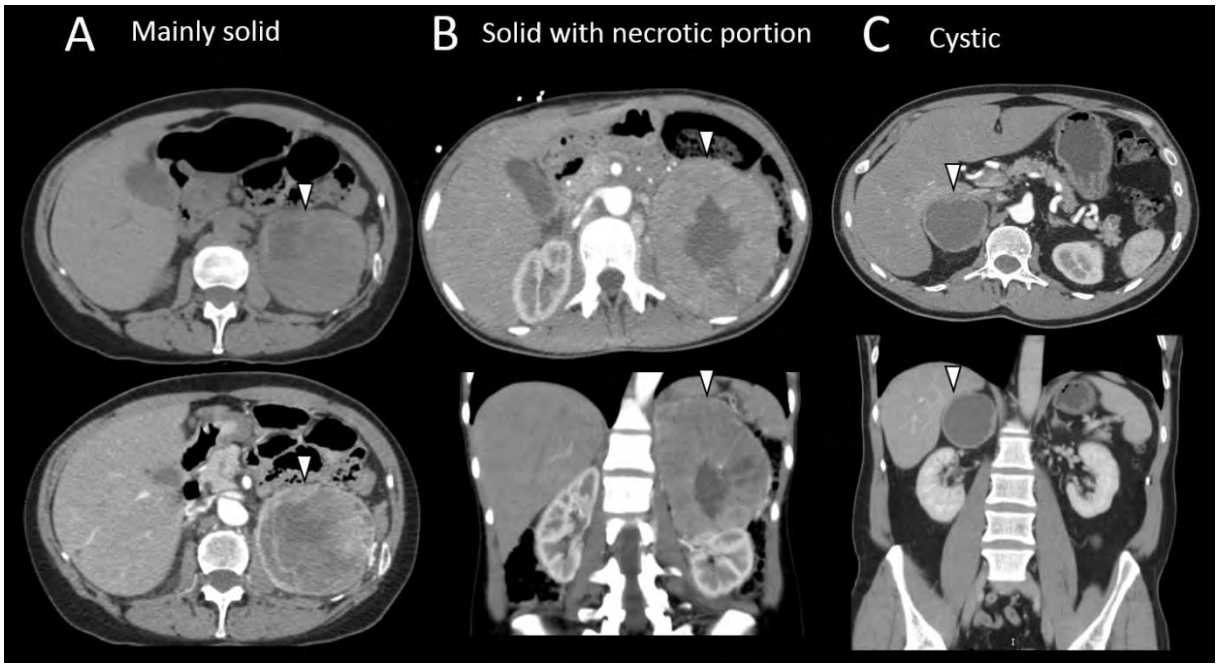

Fig. 3-*Different radiological morphologic presentation of PCCs.*

HaN PGLs : specific concerns. HaN PGLs can occur in several locations with anatomical specificities to be known for a better analysis by radiologists : carotid body 60% (angle of contact with carotid vessels), vagal nerve (osseous involvement of skull base), jugular bulb and tympanic (extension to the middle ear)[64].

Multiparametric MRI and MR angiography has a first place in diagnostic strategy of HaN soft tissue tumors, with sensitivities and specificities in HaN PGLs respectively of 90-95% and 92-99%[65]. MRI protocol should include axial T1-w sequence without fat suppression, axial T2-w fast spin-echo, and 3D T1-w contrast enhanced with fat suppression sequence.

By providing a larger anatomic coverage (from aortic arch to skull base) than conventionnal MRI sequences, contrast-enhanced MR angiography (CE-MRA) and dynamic contrast-enhanced (DCE) should also be routinely used moreover if clinical presentation evokes PGL (pulsatile mass, screening in first degree relatives): Han PGLs demonstrate early initial strong enhancement distinctive to other HaN benign lesions (arterial tumor blush), shorter time to peak followed by washout pattern (type-III curve)[66,67]. Diffusion-weighted imaging (DWI) is also in HaN PGL imaging a distinctive feature from other benign tumors, with a relatively lower apparent diffusion coefficient (ADC) (1.17 to 1.25 × 10-3 mm2/s)[66,68].

Even if DCE (based on capillary perfusion) and ADC (based on cellularity) can be considered as MRI biomarkers, no differences were observed on those parameters between sporadic and SDHx-related HaN PGLs[68].

CT and CT angiography can also be performed for diagnosis, to precise anatomical relations, but compared to MRI, CT is mainly useful to assess degree of bone destruction especially in cranial base location.

Conventional arteriography, historically used for diagnosis and localizing Han PGLs, is now reserved for embolization in few specific cases[69].

III) Molecular imaging techniques

Several molecular imaging techniques are used to diagnose and follow-up PPGLS (**Table 1**). They have diagnostic, prognostic and theranostic advantages. Among these imaging techniques, PET (positron emission tomography) imaging has a main advantage, as compared to MRI, of whole-body scanning in a single sequence.

Scintigraphy using Metaiodobenzylguanidine (MIBG). MIBG is a noradrenalin analogue with similar metabolic uptake to catecholamines. Its uptake is mediated by norepinephrine transporters, followed by vesicular storage using monoamine transporters VMAT type 1 and 2. MIBG is either labelled with ^{123}I (planar scintigraphy or SPECT/CT) or ^{131}I (planar scintigraphy) for metabolic imaging. MIBG scintigraphy has long been the gold standard for molecular imaging of PPGLs (**Fig. 4**). However, it has several limitations compared to other types of functional imaging, such as poor spatial resolution and sensitivity for small lesions due to radiotracer gamma-emission, reduced specificity due to physiologic uptake in normal adrenal glands, risk of medication interference and low uptake in malignant PPGLs. MIBG scintigraphy performance is reportedly good in PCCs and abdominal PPGLs (Se 74-97%)[70], but tends to be poor in thoracic and HaN PGLs, which are mostly V-MAT1 negative[71–73]. However, ^{123}I-MIBG scintigraphy still remains useful to assess eligibility for ^{131}I-MIBG therapy, but can also be proposed in detecting PPGL relapse after a surgery, when anatomical imaging (CT/MRI) is limited (scars, anatomical distortion, artefacts of metallic clips).

PET using dopamine analogues. Dopamine D2 receptors are membrane norepinephrine transporters predominantly expressed in sympathetic structures, which have strong avidity for mono-amines[74]. Pre-treatment with carbidopa has been shown to increase tracer uptake and increase the sensitivity of PPGLs detection[75]. Two types of Dopamine analogues are routinely used for PPGLs. ^{18}F-Fluorodopamine (FDA) is an analogue of dopamine that uses norepinephrine transporter-mediated cellular uptake. It has excellent performance for detecting and localizing PCCs in patients with known disease (Se 98%, Spe 100%)[71], metastatic PPGLs (MPPGLs)[71,76–78] and HaN PGLs including SDHx-related tumors[79]. FDA is of little help in cases of non-secreting PCC[80]. ^{18}F-dihydroxyphenylalanine (^{18}F-DOPA) is structurally similar to the dopamine precursor L-DOPA and enters neuroendocrine cells through a large amino acid transporter. Its lack of uptake in normal adrenal glands (contrary to MIBG) allows for good differentiation between a normal adrenal gland and PCC based on their respective SUVmax[81]. With sensitivity and specificity greater than 80%, ^{18}F-DOPA

is reportedly more efficient than MIBG scintigraphy[70,71,82] in detecting PPGL, especially if combined with CT/MRI[83,84]. This increased efficiency can be used to better understand biological catecholamine excess, even in patients taking medications that confound M/NM testing[85]. Currently, ^{18}F-DOPA use is mainly recommended for non-metastatic PPGLs.

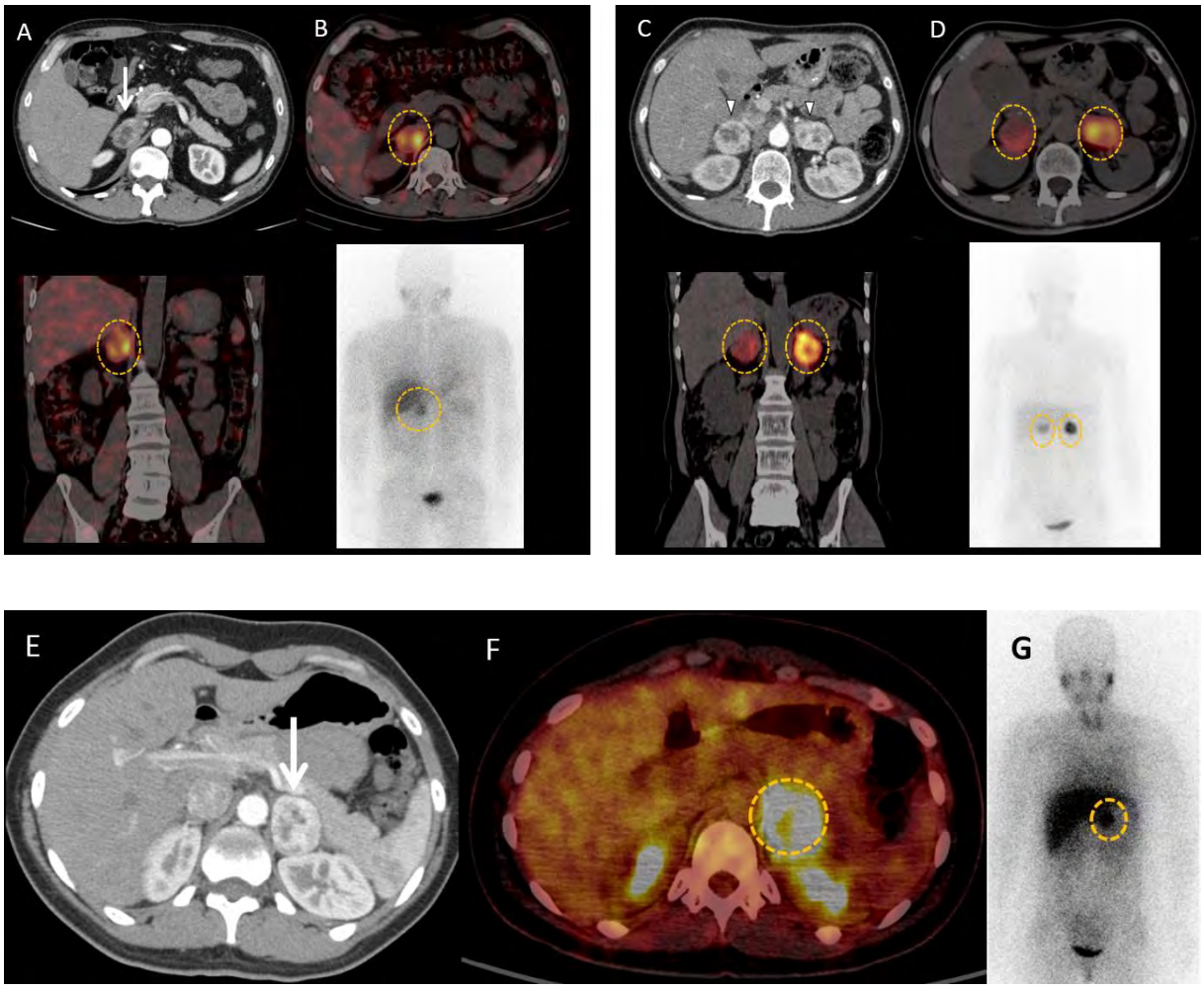

Fig. 4-*MIBG imaging in PPGLs.*

A and B 46-year-old male patient with NF1 syndrom and hypertension resistant to medications is discovered a right adrenal mass (white arrow) on CT scan (**A**). ^{123}I-MIBG scintigraphy (**B**) shows important uptake in the adrenal mass (orange circles). Adrenalectomy confirmed PCC, and induced resolution of hypertension. **C and D** 49 y.o female patient with Von Hippel Lindau syndrom is discovered bilateral adrenal masses (white arrow heads) on CT scan (**C**) with important uptake on ^{123}I-MIBG scintigraphy (orange circles) (**D**). Surgery confirmed bilateral PCCs, with no relapse at two years. **E, F and G** 39-year-old female patient with history of cervical PGL, and biological

catecholamine excess. Recent discovered of a left adrenal mass (white arrow head) on CT (**E**), showing significant uptake on ^{18}F-FDG PET (**F**) and ^{123}I-MIBG scintigraphy (orange circles) (**G**). Surgery confirmed PCC.

^{18}F-FDG PET. ^{18}F-FDG PET reportedly has poor sensitivity for detecting non-metastatic sporadic PCCs (58%), but appears to be as sensitive as ^{18}F-DOPA and better than MIBG scintigraphy for detecting MPPGLs (82%)[86–89](**Fig. 5**). Its sensitivity was also reportedly increased in SDHx and VHL related PPGLs (Se 92-99%)[88,90], and better than ^{18}F-DOPA in metastatic SDHB PPGLs[90]. In PPGLs, increased glucose uptake is not an exclusive marker of tumoral dedifferentiation, as it can also be attributed to a specific genetic defect and/or hypoxic-induced phenotype (HIF)[87]. For example, in VHL patients (including those with non-metastatic disease), the HIF pathway can induce a pseudo-hypoxic metabolic shift that increases anaerobic glycolysis, called the Warburg effect[91]. This is responsible for the high glucose uptake seen on ^{18}F-FDG PET that does not correspond to tumor differentiation.

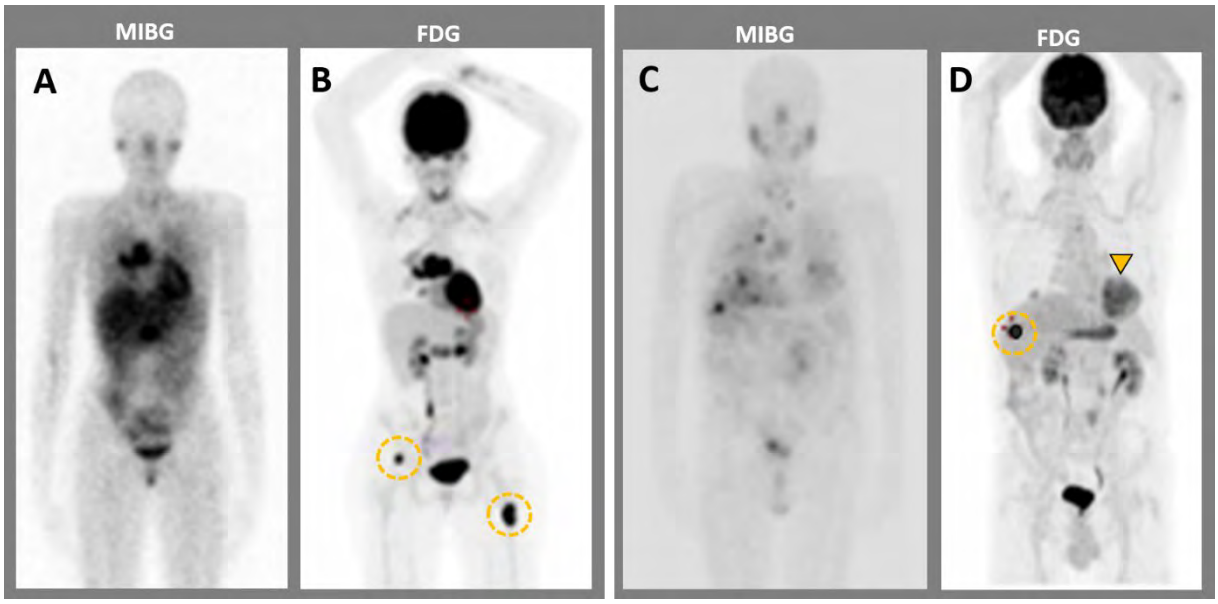

Fig. 5-*MIBG imaging vs. ^{18}F-FDG PET imaging in mPPGLs.*

A-B Patient with metastatic PCC. MIBG (**A**) has a lower sensitivity for bone metastases than ^{18}F-FDG PET (orange circles) (**B**). **C and D** Patient with metastatic PCC. MIBG imaging shows (**C**) less sensitivity for both adrenal mass (orange arrowhead) and liver metastase (orange circle) as compared to ^{18}F-FDG PET (**D**).

Scintigraphy and PET using Somatostatin analogues (SSTa). SSTa are small regulatory peptides with a high affinity for cellular somatostatin receptors (SSR). NETs usually have a high density of SSRs, explaining the tumor cells avidity for SSTa-derived agents. SSR subtypes commonly expressed in PPGLs are SSR-1 (90%), SSR-2 (70%) and SSR-3 (80%)[92]. SSTa are used in several ways: bound to a radiotracer for functional imaging or to a radionuclide for peptide receptor radionuclide therapy (PRRT), carrying out hormonal functions such as inhibition of growth hormone secretion in the pituitary and gastropancreatic systems and inhibition of tumor growth and apoptosis activation (this potential therapeutic hormonal option, already used in gastroenteropancreatic (GEP) NETs is currently being assessed in the LAMPARA study (NCT03946527) for MPPGLs[93]). Octreotide and Pentetreotide are commonly used in scintigraphy with single photon emitters (Octreoscan) and reportedly have an increased affinity for SSR-2 compared to MIBG, especially for HaN PGLs (Se97%, Spe82%)[94–99].

Radiometal positron emitting tracers, mainly represented by ^{68}Gallium (^{68}Ga) labelled with SSTa are used for PET-CT imaging. These tracers allow for an accurate initial pretherapeutic staging, early detection of relapse, and assess candidacy for therapy by using radiolabelled somatostatin analogues for metastatic nonresectable NETs (**Fig. 6**). For PPGLs, ^{68}Ga-DOTATATE imaging has become the radiotracer of choice in MPPGLs, HaNPGLs, and SDHx-related PGLs[100].

For example, in SDHB-related and sporadic PPGLs, ^{68}Ga-DOTATATE PET/CT reportedly had a 98.6% lesion-based detection rate, significantly higher than all other imaging modalities[101–103].

As far as the future of SSTa imaging, ^{18}F-SiFAlinTATE is a new PET radiotracer developed for NET imaging that appears to be a better alternative to ^{68}Ga-labelled SSTa because of its lower production cost and longer half-life[104]. However, further studies are needed to better understand its exact role in PPGLs detection and follow-up.

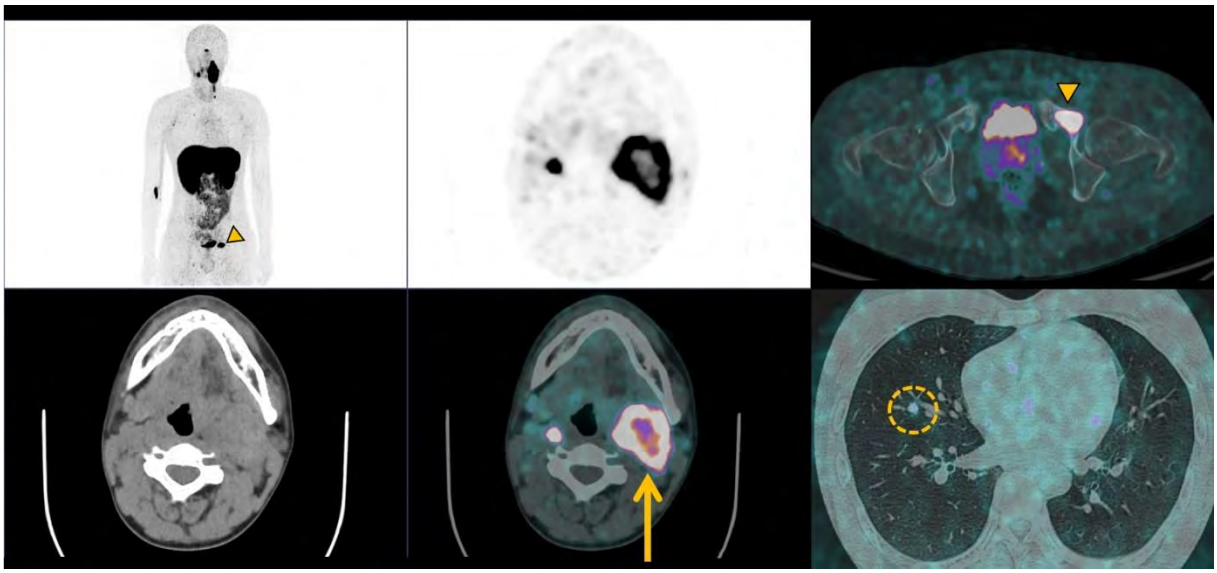

Fig. 6- *^{68}Ga-DOTATOC PET/CT in mPPGLs.*

Patient with metastatic left HaN PGL (white arrow), is proposed ^{68}Ga-DOTATOC PET imaging prior to ^{177}Lu-DOTATATE peptide receptor radiotherapy PRRT. Imaging identifies several metastases, in lung (orange circle) and bone (orange arrowhead).

Current guidelines for molecular imaging in diagnosis and staging of PPGLs. Initial molecular imaging aims to confirm the diagnosis, guide potential surgical resection, assess metastatic staging, and select patients for PRRT by choosing an appropriate modality based on the clinical context. The European Association of Nuclear Medicine Practice Guidelines[100] were updated in 2019 with an additional focus dedicated to molecular imaging and theranostics in NETs in 2021, reaching consensus for the use of ^{68}Ga-DOTA-SSTa PET/CT in staging and restaging of suspected extra-adrenal PPGLs [105].

International consensus on screening and follow-up of asymptomatic SDHx mutation carriers[106]. Early diagnose PPGLs in first-degree relatives with inherited genetic mutation is crucial, with dedicated algorithm, especially in children. During childhood, clinical (blood pressure, symptoms) and biological assessment (M/NM plasma and 24h-urinary measurements) are performed for initial screening, completed by MRI modality to reduce cumulative radiation exposure (HaN, thorax, abdomen and pelvis) rather than PET-CT (that should be performed only in adults, for initial screening step)[106]. In case of negative initial screening, follow-up is proposed clinically each year, biologically each two years, and by MRI each 2-3 years.

Future perspectives: SST antagonists. Despite a lack of internalization, SSTr subtype 2 antagonists (called BASS and JR11) were reported to provide higher tumor uptake and better tumor-to-liver background ratios than agonists. Preliminary results show improved imaging of ^{68}Ga-NODAGA-JR11 PET/CT compared to ^{68}Ga-DOTATOC PET/CT in GEP NETs. Using ^{177}Lutetium as radiotracer (^{177}Lu), higher tumor doses on PRRT can be obtained with ^{177}Lu-DOTA-JR11 compared to ^{177}Lu-DOTATE in metastasized NETs[107].

IV) Planning a surgical treatment: the role of imaging

Even though there are no curative treatments for MPPGLs, therapeutic options do exist for cases of symptomatic and/or progressive disease such as palliative surgery, systemic therapeutics, image-guided treatments and external or isotope mediated radiotherapy[108]. As we will discuss, data are scarce and large clinical trials are lacking specifically for PPGLs, because of the extremely low prevalence of metastatic cases. Instead, some therapeutics have been tested on heterogeneous NET cohorts, including those originating from different organs, despite inherent limitations.

Reminder on biopsy and PPGLs. Even if radiologists should not perform biopsy on PPGLs, this can occur in case of alternative expected diagnosis. We remind here that 24h-urinary M/NM measurements is critical before any biopsy of a lesion in anatomical localization compatible with PPGL, to prevent life-threatening outcomes[10].

Curative surgical management. Surgery is intended to be curative for non-metastatic tumors. Accurate preoperative staging, performed with both anatomical and molecular imaging, is crucial to identify anatomical risks, assess extent of disease, and discuss surgical options[45] (**Fig. 7**).

For example in HaN PGLs, Shamblin surgical classification[109] in carotid body tumors (CBT) is based on extent to carotid vessels. Pre-operative imaging criteria based on CE-CT scan or MRI, such as tumor volume, angle of contact with arterial structures, presence or absence of fat plane interface between tumor and arterial adventitia, presence of peritumoral veins, distance from skull base were reported to correlate to Shamblin group[110,111]. These findings provided to surgical team could contribute to plan surgery, predict resection difficulties and operative outcomes.

In abdominal PPGLs, laparoscopic approach is usually taken first because of its many advantages: minimally invasive, decreased blood loss and morbidity and faster recovery. However, open surgery with laparotomy is still required for large tumors or tumors closely in contact with major blood vessels (inter-aortocaval PGL or retrocaval tumor extension)[112] (**Fig. 8**). After complete resection, the risk of recurrence is estimated to be 5% over 5years of follow-up (new tumor 22%, local recurrence 23%, metastatic recurrence 55%)[113]. To improve the early detection of all types of recurrence, annual follow-up is recommended

after surgery of non-metastatic PPGL for at least 10 years after complete resection, or lifelong if there are other high-risk factors (young age, large tumor, PGL, genetic disease)[114,115].

Debulking strategy. A cytoreductive surgical approach can also be used for MPPGLs, to improve symptoms of catecholamine excess or resect a mass in a critical anatomical location [116,117]. Specifically with regards to MPPGLs, palliative surgery was reported to significantly improve median OS (148 months versus 36 months), even in patients with non-secreting tumor[117]. Furthermore, surgery could enhance the concentration of radionuclides in remaining metastatic sites, reducing tumoral burden prior to PRRT.

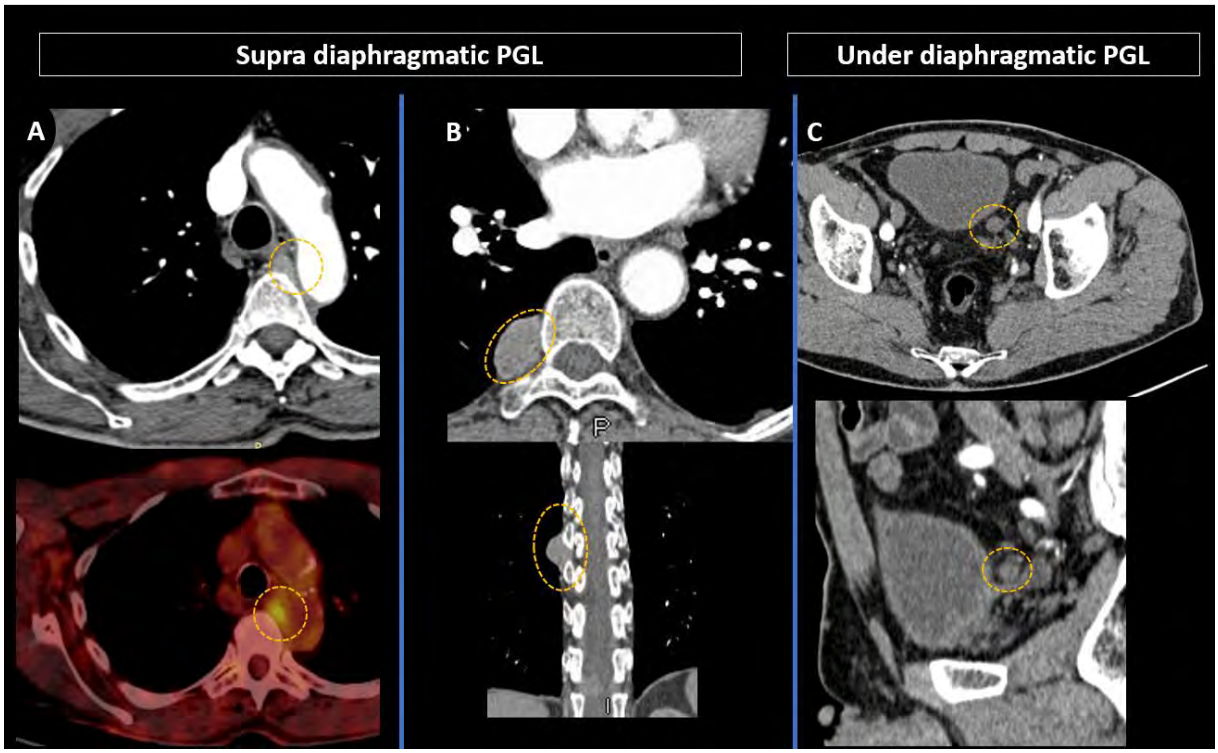

Fig. 7-*Preoperative combined anatomical and molecular imaging in PGLs.*

PGLs can develop along sympathetic chains or along glosso-pharyngeal and vagus nerve for parasymathetic PGLs, with possibility of multiple tumors in genetic syndroms. **A** Intrathoracic PGL in a 86-year-old female patient with NEM2A syndrome. **B and C** Latero-oesophageal (**B**) and and laterovesical (**C**) PGLs in a 66 year-old patient with NF1 syndrom.

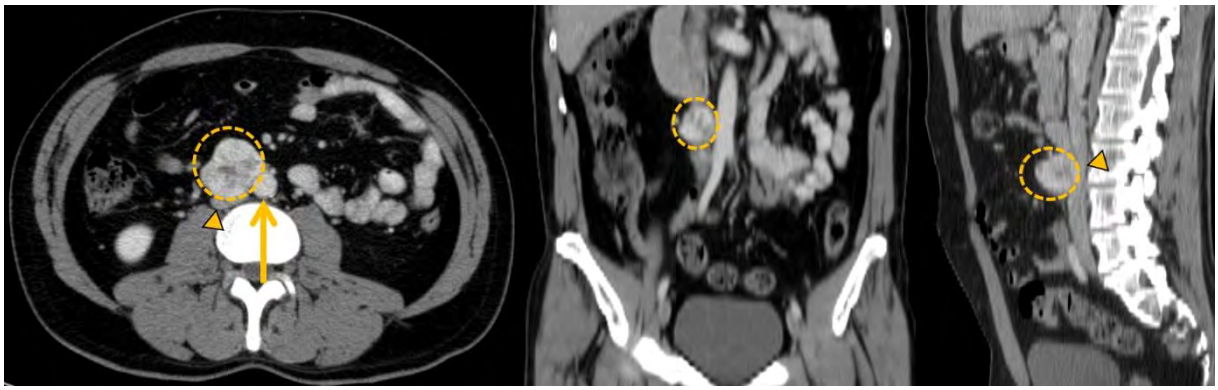

Fig. 8-*Anatomical imaging to prepare curative surgical project with vascular risks.*

Zuckerkandl organ PGL (orange circle) in a 44-year-old female patient presenting direct contact with major blood vessels (aorta : orange arrow and inferior cava vein: orange arrowhead).

V) Imaging guided therapies

Percutaneous ablation of adrenal tumors, PPGLs and metastases (mainly in bones and liver), is a safe minimally invasive treatment with short term efficacy[118,119]. There is increasing interest around ablative therapies as a palliative treatment due to their ability to reduce tumor burden and catecholamine excess in MPPGLs[120,121]. For instance, the early diagnosis and treatment of bone metastases is a therapeutic challenge, leading to more than 72% of affected patients suffering from skeletal-related events (pathological fracture, severe pain, spinal cord compression) responsible for the loss of independence or a poor quality of life[39]. Several studies report improvements in metastases-related symptoms, pain and prevention of skeletal related events (SRE) with percutaneous cementoplasty, osteosynthesis or thermal ablation[122].

Thermal ablation techniques. Several techniques are currently used for percutaneous tumor destruction[123–125]. For example, percutaneous or peroperative radiofrequency ablation (FRA) is a widespread technique[126,127] that relies on pre-operative imaging (MRI)[128]. It is based on the concept that frictional heating of the tumor results in coagulative necrosis. This procedure is frequently used on local oligometastatic liver ablations in NETs[129]. It is also used on metastatic liver lesions in MPPGLs, where it reportedly improved hypertensive symptoms and metastasis related pain[121,130]. However, based on multidisciplinary discussion, this technique is reserved for oligometastatic lesions. The expected pattern of imaging changes on follow-up is a large lesion seen on CT scan at 3 to 6 months (safety margin of ablated tissue), followed by a shrinkage of the remaining RFA-treated area with a possible remaining scar [129]. Some authors consider necrosis achieved if the lesion has no significant enhancement (<10UH) on 6 month follow-up CT[130].

Transarterial chemoembolization (TACE). Several studies have expressed interest in using TACE on the hepatic lesions of NETs to improve both OS and symptoms[131]. In MPPGLs, TACE is expected to benefit hypertension, tumor size and plasma M/NM levels[132–135]. The usual protocol involves injecting mitomycin C or epirubicin into the hepatic artery, with tumor shrinkage expected in the following months[132].

Transarterial embolization with polyvinyl or ethylene vinyl alcohol (Onyx). In HaN PGLs, polyvinyl or Onyx embolization are preoperative or palliative options that reduce blood flow to jugulo-tympanic and vagal PGLs[136], with tumor volume stability reported to be achievable

in 75% of cases at long-term follow-up[137]. For carotid body PGLs, Onyx embolization reduces blood loss and operative time, although it does make dissection more difficult [138].

Percutaneous Ethanol Injection (PEI). This imaging-guided technique was reported to be an alternative to surgery in benign PCC by inducing necrosis and reducing tumor size[139]. It is also of interest in treating metastases[120]. However, there is a clear need for comparative studies and further data to assess the benefit of percutaneous ablative techniques on OS.

External Radiotherapy: role of imaging . For HaN PGLs (temporal bone, carotid body, and/or glomus vagal) and intra-thoracic PGLs, RT is an alternative to surgery, especially when tumor resection would cause neural and vascular damage in cases of extensive spread. Surgical resection of jugular and vagal PGLs generates significantly more cranial nerves palsies and major complications with less tumor control compared to radiotherapy, suggesting that surgery should be considered only for selected cases[140,141]. In MPPGLs, external beam radiation therapy (EBRT) is also useful in obtaining local control and improving symptoms[142,143]. Anatomical imaging (especially head and neck MRI), and molecular imaging are crucial in order to adapt the radiation field to limit radiation-induced complications (xerostomia, neural deficits, osteonecrosis), and for post-treatment follow-up. Expected findings on imaging are growth control (mainly progression control, or reduction in size) and decrease in vascularity rather than tumor elimination[142].

VI) Systemic therapies: impact of new therapeutics in imaging management[33,115,144]

Several concepts are used in support of systemic therapies for PPGLS. These therapies are intended to have an anti-progression effect (as chemotherapy), a symptomatic effect (by managing catecholamine excess with metyrosine and other anti-hypertensive medications) and pain reduction. Several types of systemic therapies are used for PPGLs (**Table 2**).

Cytotoxic therapies. The classic cytotoxic chemotherapies cyclophosphamide, vincristine and dacarbazine, known as the CVD-protocol, can be used to treat PPGLS. They tend to decrease catecholamine excess and reduce tumor and lymph node size in 30 to 70% of patients[145–148]. The clinical benefit to overall survival in MPPGLs is unclear, even if research has reported longer mean survival in responders (3.8 years) compared to non-responders (1,8 years)[146]. Alternatives to the CVD-protocol have become first line treatment options, such as temozolomide, which provides a significantly longer PFS in SDHB-mutated-MPPGLs compared to other MPPGLs[149]. As with other NETs, assessing treatment response to cytotoxic drugs using anatomic imaging with RECIST is limited by the slow-growing behavior of PPGLs. Therefore, a decrease in size is rarely achieved in NETs, even for patients with the best survival rates [149–152]. Tumor contrast enhancement response patterns in CT and MRI imaging reportedly not useful for response assessment to cytotoxic therapies. Moreover, radiologists should be aware that contrast medium injection protocols could interfere with tumor size measurements[150], thus biasing image interpretation[153].

Targeted therapies. Several targeted therapies, such as Tyrosine kinase inhibitors (TKI) and Interferon alpha biotherapy[154] are also in use. For instance, sunitinib (TKI) has become a first-line option in MPPGLs, inducing decreased tumor size and improvement in hypertension[155,156], and has recently provided promising results in PFS at 12 months (ongoing clinical trial FIRSTMAPP)[157]. Interferon alpha has also shown improved disease stabilization[154]. Even if *SSTa* has a significant effect on hormone levels in GEP NETs[158,159] with decreased symptoms of flushing and diarrhea, their use in PPGLs is currently not being investigated. As most targeted agents are cytostatic, there is need for image-based criteria to assess tumor response. For example, perfusion CT's ability to describe the change in tumor density of hypervascular NETs is of interest[152,160]. This could also apply to PPGLs since they are hypervascular slow-growing tumors, however further comparative studies are needed.

Immune Checkpoint Inhibitors (ICIs). Although the use of ICIs for NETS still has not been approved, they are currently under investigation in clinical trials. For MPPGLs, pembrolizumab was recently reported to induce a 43% non-progression rate and a 75% clinical benefit rate (CBR) at 27 weeks[161]. Due to their distinct effect on anti-tumor immunity, there are many well-documented immune-related phenomena associated with ICI use. Several new patterns of tumor response and progression (pseudo-progression, hyper-progression, abscopal effect), as well as adverse events are widely described in the literature and are important for radiologists to know, because they can lead to misdiagnoses[162–168]. In fact, detection of immune related adverse events (iRAE) in patients treated with ICIs is a crucial challenge for radiologists[169]. They can occur at any site during patients' treatment with ICIs, and mainly affect the endocrine glands (hypophysitis, thyroiditis, hepatitis, pancreatitis), lung and mediastinal lymph nodes, digestive tract (enterocolitis) and joints (arthralgia).

Taking these aspects into consideration, these therapeutics bring more challenges to medical imaging interpretation. For instance, iRECIST and iPERCIST criteria should be used for ICIs[106]. iRECIST introduces the concepts of immune unconfirmed progressive disease iUPD, which states that an increase in the size of a lesion or the appearance of new lesions should be closely followed up on by subsequent imaging. If on the next radiological examination there is no change in the size or appearance of the tumor, then it remains as iUPD. However, if the size increases then it is classified as immune confirmed progressive disease (iCPD). A decrease in size is classified as conclude response (iCR, iPR). Also developed for ICIs, the iPERCIST (immune PET response criteria in solid tumors) criteria is a modified classification system that takes into consideration a novel type or tumor response based on a dual-time-point, called unconfirmed progressive metabolic disease (UPMD), which helps to limit false interpretations. If confirmed at a repeat scan 3-4 weeks later, the tumor is classified as confirmed progressive metabolic disease (CPMD). In non-small cell lung cancer, one third of UPMD were later classified as SMD or PMR (stable or partial metabolic response), thereby using iPERCIST to provide prognostic information[170].

VII) Targeted Radionuclide Therapies (TRT)

Rationale. These molecular imaging-based modalities take advantage of the fact that peptide-linked radiotracers can target membrane-bound receptors. The two main purposes of these include: 1) confirming sufficient radiotracer affinity to the tumor and 2) binding to the specific membrane receptor, which allows internalization into the tumor and can emit radiation that leads to DNA damage and apoptosis. With a low antigenicity, rapid tissue penetration, and fast blood clearance, a relatively easy and less expensive method of synthesis compared to monoclonal antibodies, are an effective alternative to chemotherapies and with less side effects. Their use is mostly in patients with inoperable or metastatic NETs.

Iobenguane or ^{131}I-MIBG. This therapeutic is reported to improve symptoms from catecholamine excess in over 40% of MPPGLs patients, and induce a mean progression-free survival of 23.1-28.5 months for common and mild adverse events[171–173]. The expected radiologic pattern of response is mainly SD (stable disease) or PR (partial response) on CT scan[171], and a lower MIBG uptake (**Fig. 9**). Therapy with higher delivered doses of ^{131}I-MIBG has been reported to have higher 5 years-OS, but should be reserved for selected patients because of increased adverse events (pulmonary toxicity, myelosuppression, myelodysplasia, leukemia)[174].

Peptide receptor radiotherapy PRRT. The key concept behind this therapeutic approach is that a radionuclide can bind a peptide that specifically targets a cellular receptor[175–177]. Specific data in patients with PPGLs are scarce, but an ongoing clinical trial is assessing PRRT in inoperable PPGL, with the results expected in 2023 (NCT03206060). ^{90}Yttrium in ^{90}Y-DOTATOC is also reportedly effective on response rate (morphological response in 10-40% of patients [178]), survival time and symptomatic response in NETs, with limited adverse events [179,180]. *^{177}Lu-DOTATATE,* considered a third generation SSR-PRRT, has the advantage of increased affinity for octreotate compared to octreotide on SSR positive tissues, allowing longer tumour residence [181] for a higher tumor absorbed dose and promising results in PFS for GEP-NETs[182]. As compared to ^{90}Y, the main advantage of ^{177}Lu is that it is not a pure beta-emitter, it also emits low energy gamma-rays, allowing for post-therapy SPECT imaging and dosimetry. The NETTER-1 trial is also worth mentioning here, even though it was performed in midgut NETs, because it is the only randomized phase III clinical study offering high level evidence of efficacy with ^{177}Lu-DOTATATE on PFS and response rate[183]. In HaN PGLs, ^{177}Lu-DOTATATE was also reported an adequate alternative for achieving

PR or SD in cases where surgery or radiation were contraindicated due to local neurovascular structures[184]. According to the 2019 NANETS/SNMMI Consensus Statement[185], ^{177}Lu-DOTATATE in MPPGLs is promising but can induce long-term complications such as therapy-related myeloid neoplasms[186]. Additionally, any imaging pattern associated with this treatment was not studied[178]. This treatment should be limited to MIBG-negative patients, whereas MIBG-positive patients may preferentially undergo ^{131}I-iobenguane therapy.

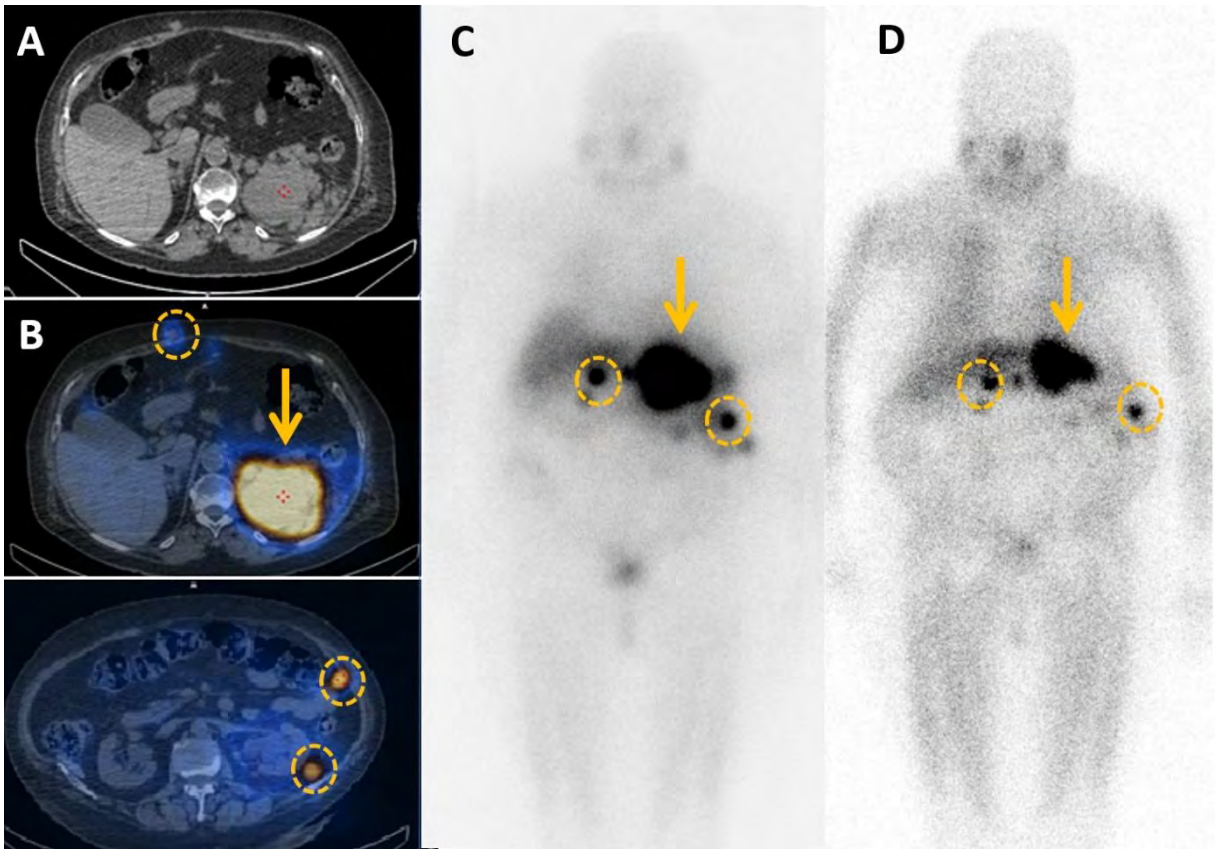

Fig. 9-*Metabolic imaging in mPPGLs for local and systemic extension.*

Patient treated for a 13cm-diameter left PCC by surgery is diagnosed nine years later a 8cm-diameter mass on CT (**A**). MIBG imaging confirms local relapse (**B**) (orange arrow), but also subcutaneous and peritoneal metastases (orange circles). Debulking strategy would be too aggressive, so ^{131}I-MIBG therapy is proposed. Post-therapy MIBG scintigraphy (**C**) shows a reduced size of the mass and peritoneal implants, and lower MIBG uptake compared to pre-therapeutic MIBG scintigraphy (**D**).

VIII) Tumor response management: new concepts and pitfalls

MPPGLs are slow growing and heterogeneous, which has important implications for diagnosis and management.

First, baseline imaging is crucial in assessing disease-extent, planning treatment, and guiding further management in order to reduce long-term treatment side effects. Second, RECIST 1.1 does not accurately assess early tumor response, and a more precise and reliable set of guidelines is needed[187]. One potential alternative, computer science, uses semi-automated measurements such as advanced segmentation, can provide quantitative analysis by recognizing and delineating a lesion, which provides an estimate of tumor volume or can calculate tumor burden. Third, performing several imaging modalities (by combining anatomical and molecular imaging) on a heterogeneous tumor can be useful for follow-up. Fourth, if a new highly sensitive imaging modality (i.e., new PET tracers) that was not used at baseline shows new lesions, they should be considered "new baseline lesions" for this imaging modality instead of disease progression. Although there is a high chance these lesions existed before, they should only be counted when detected. Finally, considering that these tumors are slow growing and most of their treatments are “non-cytoreductive”, disease nadir and baseline tumor burden should be incorporated into management.

RECIST 1.1 limitations [188]. These quantitative size-based radiological criteria are used for therapy response assessment with standardized choice and target lesions quantification. Several situations can lead to non reproductible measures including irregular lesions with complex shapes, bone lesions, fibrosis or necrotic lesions with unprecise limits, variability of behavior of lesions for a same patient, arbitrary selection of target lesion leading to imprecise therapeutic response evaluation and slow growing tumor. Additionally, some new classes of treatment provide mechanisms and patterns of response that are not size-assessable. For example, ICIs can induce an effective but delayed response, or behave like a progressive lesion because of an initial immune-mediated flare in size. Antiangiogenic agent can also induce hemorrhage, necrosis, myxoid degeneration with a possible early transitory increase in size[189].

Molecular Imaging Reporting and Data System (MI-RADS) in SSTR: the SSTR-RADS

SSTR-targeted radiotracers allow specific imaging of SSTR-avid structures with some limitations (normal organs uptake, urinary excretion, inflammatory diseases…) that should

be known by radiologists[176]. SSTR-RADS is the first PET classification system based on tumor uptake and uses a reliable five point scale that can assess treatment response and identify ideal candidates for PRRT from poor responders[190,191].

IX) Discussion: Theranostics in PPGLs, current and future perspectives in the era of artificial intelligence

As with other NETs, PPGLs are highly heterogeneous neoplasms, with many variations at the genetic, cellular, molecular, functional, clinical and histopathological level. In order to create more tailored treatments, these different variables need to be understood as a global interrelated system. The fact that there is such genetic and phenotypic heterogeneity suggests that there is potential to develop personalized treatments. For example, predictive biomarkers could be used to identify patients most likely to respond to treatment, assess the effectiveness of PRRT in MPPGLs for protocol adjustment, or help choose alternative/combined treatments with optimal cost/benefit[192,193].

Imaging and radiomics biomarkers[194]. Several anatomical biomarkers can be used to improve tumor monitoring, and others are still under testing (**Table 3**). *Tumor Growth Rate (TGR)* in GEP-NETs was reportedly an early predictor of PFS[195,196] because it revealed a large proportion of patients with active tumor growth despite classification as SD according to RECIST 1.0. This was especially true during early treatment response evaluation. *Volume assessments for early detection of change* provides better inter-operator agreement compared to measuring the long tumor diameter according to RECIST, which leads to better detection of early partial responders versus progressive disease[197]. Recently, a dedicated mathematical model based on shape, margin, necrosis and ring sign, has been proposed to improve the diagnosis of PCCs in front of an undetermined adrenal mass. Based on imaging characteristics on unenhanced CT such as sharp-edged necrosis, unsharp necrosis, ring sign and spherical shape, a predictive calculation model had good specificity and sensitivity (80%/95%) for diagnosing PCCs[198]. Machine learning-based quantitative texture analysis (QTA) of unenhanced CT scans was also recently proposed, which can help differentiate subclinial PCCs from lipid-poor adenomas. The texture analysis was based on 30 texture features that went into an equation for differentiating the two tumor types[199,200].

SPECT / PET metabolic biomarkers mainly assess tumor burden based on volumetric lesion segmentation. Several parameters are indicators of prognostic value. SUV mean, SUV max, Metabolic Tumor Volume (MTV) and Total Metabolic Tumor Volume (TMTV). These are easily extracted biomarkers obtained using traditional visualization software, reportedly associated with overall survival (OS), PFS, response prediction[201].

At the voxel level, textural features (TF) such as entropy, homogeneity and intensity variation have been proven to correlate with tumor aggressiveness. They are also of interest for risk stratification. In GEP-NET patients undergoing pre-treatment SSTR-PET CT, entropy and intensity may predict OS[202].

Metabolomics. Metabolomics or metabolite profiling is the comprehensive analysis of small molecule metabolites to assess phenotypic and genetic characteristics of a lesion. It links molecular genetics concepts to imaging. Several new markers are described in the literature. Magnetic Resonance Spectroscopy (MRS) for in vivo metabolomics is a highly promising field. For instance, 1H-MRS SUCCES (SUCCinate Estimation by Spectroscopy) detects succinate concentrations in order to non-invasively measure mutations in the biomarker SDHx. Succinate concentration can be increased up to 100 times compared to non-SDHx mutated PGLs, which allows for detection of in vivo SDH deficiency in most PPGL patients. This technique has limitations for those with a small tumor, hemorrhagic or necrotic spots or respiratory motion on imaging. This modality could allow for early detection of SDH deficiency in routine clinical practice, quicker than genetic tests, with a positive impact on management and clinical outcomes. It could prompt a search for tumor SDHx mutations in cases of negative germline genotyping with a positive succinate peak and detect it before surgery or confirm a suspicious lesion as metastatic. Furthermore, in the setting of a suspected SDHx mutation, a known predisposition to other tumors such as GIST could optimize CT/MRI imaging analysis[203–206] (**Fig. 10**).

Genomic and methylomic. At the genome-scale, DNA methylation is a major way of regulating gene transcription and phenotype expression. Hypermethylation in promoted gene regions can induce gene silencing, with possible pro-oncogenic shift of regulation pathways. Recent findings indicate that methylome remodeling caused by SDHx mutations results in major transcriptional abnormalities with significant impact on epigenetics features. This makes methylome and transcriptome new biomarkers of interest directly linked to phenotypic features such as metastatic or reccurence and various survival rates depending of methylation clusters[207]. In NETs for example, the NETest is a 51 multigene assay performed by 4 different prediction algorithms based on PCR analysis of a peripheral blood sample of specific NET circulating transcripts. This reflects real-time tumor activity and was reportedly of prognostic value since it was associated with response type to SSA-PRRT[208] or diagnosing progression of disease one year earlier than image-based evidence[209]. In

PPGLs specifically, integrated bioinformatics analysis based on microarrays identified in PCCs has found disease-causing genes of diagnostic, prognostic, and therapeutic value (good prognosis for KCNH2, KCNQ2, KCNQ1; poor prognosis SCN2A)[210,211].

MiRNAs physiologically regulate gene expression by targeting mRNAs to induce their degradation and/or repression. In PPGLs, miRNome datasets identified alterations and miRNA signatures of prognostic value. Six miRNAs (miR-21-3p, miR-183-5p, miR-182-5p, miR-96-5p, miR-551b-3p, and miR-202-5p) were predictive of shorter time to progression and associated with metastatic risk in PPGLs[212].

Conclusion

In this comprehensive review, we aimed to discuss the current state of the art medical imaging for PPGLs diagnosis and treatment. Despite major medical improvements, PPGLs, as with other NETs, leave clinicians facing several challenges, due to their inherent particularities. The conventional concepts of medical imaging are currently undergoing a paradigm shift, thanks to developments in artificial intelligence (AI). However, despite currently active research in the fields of radiomics, metabolomics and new biomarkers, the clinical relevance of these new parameters remains unclear and further multicentric studies are needed in order to increase generalizability. Use of AI in PPGLs may detect changes in tumor phenotype that precede classical medical imaging biomarkers, such as size. Multicentric data aggregation in PPGLs disease will be necessary for PPGLs management because of their scarcity, slow growth, high heterogeneity and long overall survival. Moreover, medical imaging data can be implemented in hybrid models combining genomics and transcriptomics which can then be mined by Artificial Intelligence in hopes of finding new biomarkers to improve patients' overall management.

Dans cette revue bibliographique, nous avons cherché à faire la synthèse des données actuelles sur les modalités d'imagerie des PPGLs à visée diagnostique et de suivi. Malgré des avancées médicales majeures, les PPGLs, comme les autres NETs, présentent des spécificités phénotypiques que le radiologue doit connaître. Les concepts actuels en imagerie médicale connaissent un changement de paradigme, grâce à une meilleure compréhension des spécificités en imagerie (notamment métabolique) de ces tumeurs et à l'apport de l'intelligence artificielle. Cependant, malgré les recherches actuelles en cours dans les domaines de la radiomique, metabolomique et d'identification de nouveaux biomarqueurs, l'apport clinique de ces nouveaux paramètres reste à préciser, et de futures études multicentriques sont nécessaires pour en permettre l'applicabilité. L'utilisation de l'IA pour les PPGLs pourrait par exemple détecter des changements dans le phénotype tumoral précédent les modifications des biomarqueurs classiquement utilisés en imagerie. Du fait de la rareté, la croissance lente, l'importante hétérogénéité en imagerie des PPGLs, des analyses multicentriques seront nécessaires en confrontant données d'imagerie, génomique et transcriptomique dans des modèles hybrides d'IA à la recherche de nouveaux biomarqueurs pertinents pour la prise en charge globale du patient.

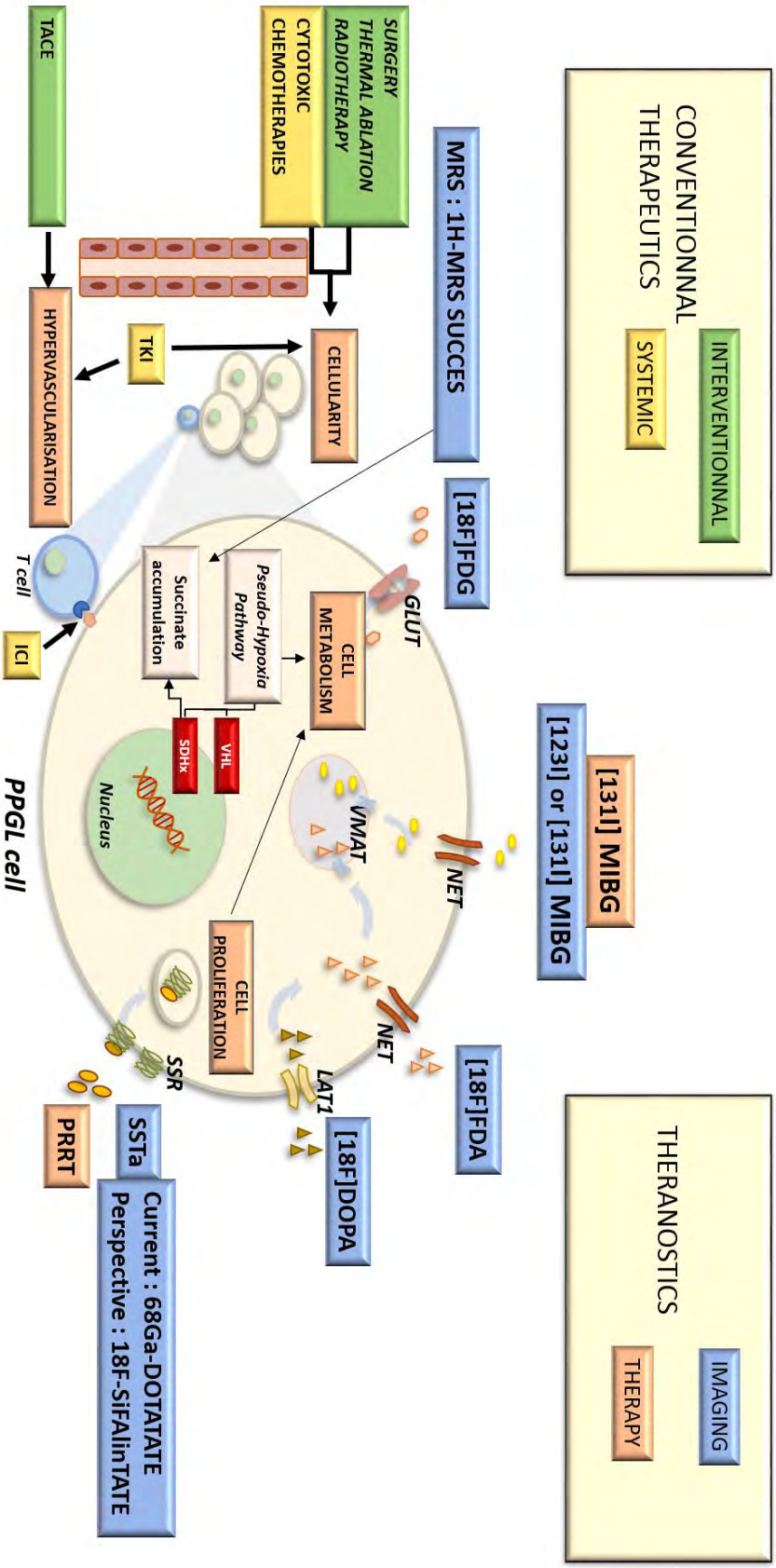

Fig. 10-*Theranostic in PPGLs: a multidisciplinary approach.*

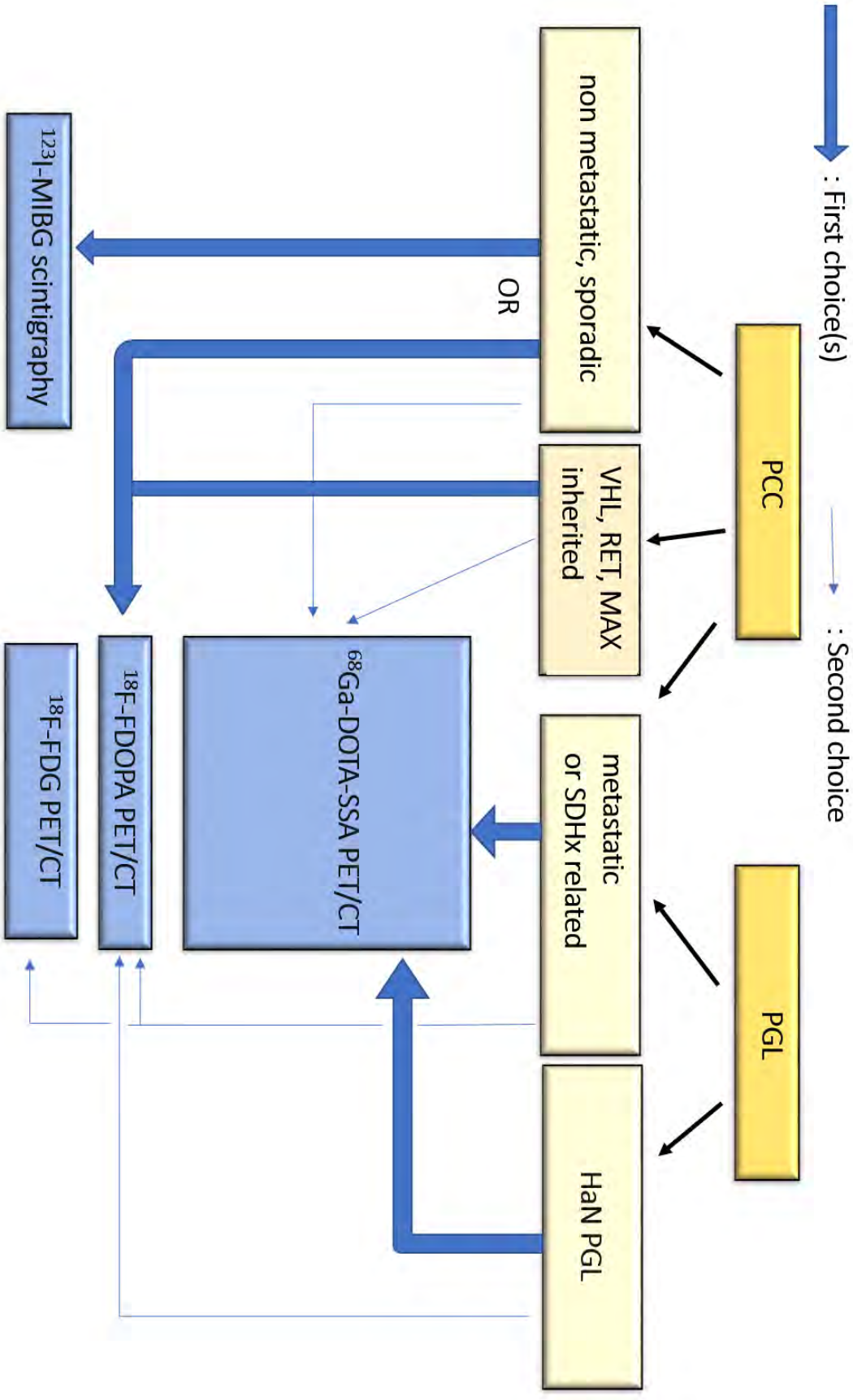

Fig. 11-*Current guidelines for molecular imaging in diagnosis and staging of PPGLs.*

	Name	Advantage	Mechanisms of action	Performances	Disadvantages, adverse events
SSTa	^{68}Ga-DOTATATE	detect lesions with negative MIBG scintigraphy in PPGLs[103,213,214]	good affinity for SSR-2, SSR-3 and SSR-5[216]		Lack of availability worlwide
	^{68}Ga-DOTANOC	-detection of NETs metastasis -more efficient in comparison to ^{18}F-DOPA [215]		100% Se and Spe[217]	
	^{68}Ga-DOTATOC	-good sensibility for metastatic PCCs-detection of NETs bone metastases [218]		(92%)[219]	
	^{68}Ga-DATATOC	easier and quicker preparation of the radiopharmaceutical tracer than DOTA. [220]		to be determined	
MIBG	^{123} or ^{131}I-MIBG	Assessment prior to ^{131}I MIBG therapy Better analyse than CT/MRI when anatomical distorsion (post-surgery, scars, metallic clips)	Analog of guanethidine, cellular uptake by NET	Se 74-97% in PPGL (lower if metastatic) except thoracic and HaN PGL : poor	Physiological uptake in adrenal gland Drug interactions
FDA/FDOPA		Low uptake in normal adrenal gland	FDOPA is a precursor of FDA in catecholamine synthesis, cellular uptake by LAT1, decarboxylated into FDA	Se and Spe superior to 90%	Lower sensibility in MPPGLs and SDHx-related PPGLs
FDG		poor sensitivity for non-metastatic sporadic PCCs (58%)	FDG is a surrogate of glucose, with a cellular uptake mainly by GLUT1	Better than MIBG scintigraphy, in MPPGLs (82%) High sensitivity in SDHx patients	Lack of specificity for PPGL and PCC

Tab 1-*Metabolic imaging radiotracer used for imaging techniques.*

	Target	Cellular clinical effects	Radiological patterns of response	Clinical benefits, ongoing trials
Chemotherapy	CVD-protocol: cyclophosphamide, vincristine and dacarbazine	catecholamine excretion reduction?	decrease in size	- catecholamine excess improvement (30-40% of patients) -unclear benefit on overall survival in MPPGLs for several adverse events[145–147] LAMPARA trial (NCT03946527), assessing Lanreotide in MPPGLs
SSTa therapies		tumor cells growth inhibition apoptosis activation		significant improvement of clinical symptoms (flush, diarrhea) in GEP NETs[158,159]
Interferon alpha	natural killer lymphocyte functions stimulation		growth control (stable disease)	clinical improvement of pain, headaches, paradoxical diarrhea, sweating
Tyrosine kinase inhibitors (TKI)		anti-neoangiogenic, pro-apoptotic, inhibitor of cell growth and cell migration	decrease in size[155,160] diminution of glucose uptake[156] PFS improvement[157]	- Sunitinib : FIRSTMAPPP trial NCT01371201 - Axitinib: NCT01967576 - Cabozantinib: NCT02302833
Immune checkpoint inhibitors (ICI)	- CTLA-4: ipilimumab - PD-1: nivolumab, pembrolizumab - PD-L1: aterolizumab, avelumab, durvalumab	- tumor reduction - hormonal secretion reduction in MMPPGLs	pseudoprogression hyperprogression abscopal effect	NCT02721732: rare tumors including MPPGLs
PRRT	^{90}Y-DOTATOC	limited adverse events (nausea, reversible hematopoietic toxicity)[179,180]	-good sensibility for metastatic PCCs - detection of NETs bone metastases [218] - morphological response[178]	symptomatic response (pain, carcinoid syndrome)
	^{177}Lu-DOTATATE		^{177}Lu-DOTATATE in mPPGLs is promising but should be limited to MIBG-negative patients[185]	^{177}Lu is not a pure beta-emitter, but also emits low energy gamma-rays, allowing post-therapy imaging and dosimetry ongoing clinical trial (NCT03206060) PRRT in inoperable PPGL (^{177}LuDOTATE for PCCs and ^{68}GaDOTATATE for PGLs)
Iobenguane or ^{123}I-MIBG[171–173]			reduction in size on CT scan, and a lower MIBG uptake[174] In HaN PGLs, potential alternative when neurovascular structure location is a contraindication to surgery or radiation therapy, to achieve PR or SD[184]	β- particle and γ-radiation by nuclear transformation

Tab 2-*Systemic and theranostic therapies.*

		Imaging modality/ calculation method	Advantage
Anatomical imaging	Tumor Growth Rate TGR	2D on CT scan, as the percentage change in tumor size over one month (%/m)	early predictor of PFS [195,196]
	Volume assessments for early detection of change	3D on CT scan, volume measurement	better inter-operator agreement, earlier partial response or progressive disease[197]
SPECT / PET metabolic biomarkers	SUV max	2D on PET CT	- in advanced (NSCLC)significantly predictive of response to anti-PD-1 antibody -from pretherapeutic ^{68}Ga-DOTATOC-PET/CT for NET, predictive of response probability of PRRT.therapy[196,197]
	Metabolic Tumor Volume (MTV)	a margin threshold of x% of SUVmax	pancreatic NETs: predictor of overall survival[223]
	Total Metabolic Tumor Volume (TMTV)	3D	advanced NSCLC or melanoma treated with ICIs, high TMTV from pre-treatment ^{18}F-FDG PET was associated with shorter PFS, -risk stratify patients with different overall survival probabilities[224,225]
	Somatostatin Receptor Expressing Tumor Volume (SRETV, mL) and Total Lesion Somatostatin Receptor Expression (TLSRE, g)	^{68}Ga-DOTATATE PET/CT, 3D	significant and independent prognostic value in well-differentiated NETs on PFS[176]
Radiomics	Asphericity (ASP)	^{111}In-octreotide scintigraphy prior to PRRT imaging-based quantification of lesion's spatial heterogeneity with an automatic algorithm for delineation	GEP-NETs response prediction : higher ASP was significantly associated with worse response[226]
	Textural features (TF):	2D and 3D, voxel level entropy, homogeneity, intensity variation…	In GEP-NET patients undergoing pre-therapeutic SSTR-PET CT, entropy and intensity were significant predictors of OS[177].

Tab 3-*Imaging biomarkers currently used in PPGLs.*

Bibliography :

1. Motta-Ramirez, G. A., Remer, E. M., Herts, B. R., Gill, I. S. & Hamrahian, A. H. Comparison of CT Findings in Symptomatic and Incidentally Discovered Pheochromocytomas. *Am. J. Roentgenol.* **185**, 684–688 (2005).
2. Kim, J. H., Moon, H., Noh, J., Lee, J. & Kim, S. G. Epidemiology and Prognosis of Pheochromocytoma/Paraganglioma in Korea: A Nationwide Study Based on the National Health Insurance Service. *Endocrinol. Metab.* **35**, 157 (2020).
3. Pacak, K., Linehan, W. M., Eisenhofer, G., Walther, M. M. & Goldstein, D. S. Recent Advances in Genetics, Diagnosis, Localization, and Treatment of Pheochromocytoma. *Ann. Intern. Med.* **134**, 315 (2001).
4. Berends, A. M. A. *et al.* Incidence of pheochromocytoma and sympathetic paraganglioma in the Netherlands: A nationwide study and systematic review. *Eur. J. Intern. Med.* **51**, 68–73 (2018).
5. Currás-Freixes, M. *et al.* Recommendations for somatic and germline genetic testing of single pheochromocytoma and paraganglioma based on findings from a series of 329 patients. *J. Med. Genet.* **52**, 647–656 (2015).
6. Jain, A., Baracco, R. & Kapur, G. Pheochromocytoma and paraganglioma—an update on diagnosis, evaluation, and management. *Pediatr. Nephrol.* **35**, 581–594 (2020).
7. Lenders, J. W., Eisenhofer, G., Mannelli, M. & Pacak, K. Phaeochromocytoma. *The Lancet* **366**, 665–675 (2005).
8. Timmers, H. J. L. M. *et al.* Clinical Presentations, Biochemical Phenotypes, and Genotype-Phenotype Correlations in Patients with *Succinate Dehydrogenase Subunit B* -Associated Pheochromocytomas and Paragangliomas. *J. Clin. Endocrinol. Metab.* **92**, 779–786 (2007).
9. Yokomoto-Umakoshi, M. *et al.* Pheochromocytoma and paraganglioma: An emerging cause of secondary osteoporosis. *Bone* **133**, 115221 (2020).

10. Vanderveen, K. A. *et al.* Biopsy of pheochromocytomas and paragangliomas: Potential for disaster. *Surgery* **146**, 1158–1166 (2009).

11. Eisenhofer, G. *et al.* Biochemical Diagnosis of Pheochromocytoma: How to Distinguish True- from False-Positive Test Results. *J. Clin. Endocrinol. Metab.* **88**, 2656–2666 (2003).

12. Bílek *et al.* Chromogranin A in the Laboratory Diagnosis of Pheochromocytoma and Paraganglioma. *Cancers* **11**, 586 (2019).

13. Plouin, P. F. *et al.* European Society of Endocrinology Clinical Practice Guideline for long-term follow-up of patients operated on for a phaeochromocytoma or a paraganglioma. *Eur. J. Endocrinol.* **174**, G1–G10 (2016).

14. Benn, D. E. & Robinson, B. G. Genetic basis of phaeochromocytoma and paraganglioma. *Best Pract. Res. Clin. Endocrinol. Metab.* **20**, 435–450 (2006).

15. Brunt, L. M. *et al.* Adrenalectomy for Familial Pheochromocytoma in the Laparoscopic Era: *Ann. Surg.* **235**, 713–721 (2002).

16. Pollard, P. J. *et al.* Expression of HIF-1α, HIF-2α (EPAS1), and Their Target Genes in Paraganglioma and Pheochromocytoma with *VHL* and *SDH* Mutations. *J. Clin. Endocrinol. Metab.* **91**, 4593–4598 (2006).

17. Waldmann, J. *et al.* Mutations and polymorphisms in the SDHB, SDHD, VHL, and RET genes in sporadic and familial pheochromocytomas. *Endocrine* **35**, 347–355 (2009).

18. Dluhy, R. G. Pheochromocytoma — Death of an Axiom. *N. Engl. J. Med.* **346**, 1486–1488 (2002).

19. Qin, Y. *et al.* Germline mutations in TMEM127 confer susceptibility to pheochromocytoma. *Nat. Genet.* **42**, 229–233 (2010).

20. Fishbein, L. *et al.* Comprehensive Molecular Characterization of Pheochromocytoma and Paraganglioma. *Cancer Cell* **31**, 181–193 (2017).

21. Astuti, D. *et al.* Gene Mutations in the Succinate Dehydrogenase Subunit SDHB Cause Susceptibility to Familial Pheochromocytoma and to Familial Paraganglioma. *Am. J. Hum. Genet.* **69**, 49–54 (2001).

22. Gimenez-Roqueplo, A.-P. *et al.* Mutations in the SDHB gene are associated with extra-adrenal and/or malignant phaeochromocytomas. *Cancer Res.* **63**, 5615–5621 (2003).

23. Ricketts, C. J. *et al.* Tumor risks and genotype–phenotype–proteotype analysis in 358 patients with germline mutations in *SDHB* and *SDHD*. *Hum. Mutat.* **31**, 41–51 (2010).

24. Hamidi, O. *et al.* Outcomes of patients with metastatic phaeochromocytoma and paraganglioma: A systematic review and meta-analysis. *Clin. Endocrinol. (Oxf.)* **87**, 440–450 (2017).

25. Zelinka, T. *et al.* Role of positron emission tomography and bone scintigraphy in the evaluation of bone involvement in metastatic pheochromocytoma and paraganglioma: specific implications for succinate dehydrogenase enzyme subunit B gene mutations. *Endocr. Relat. Cancer* **15**, 311–323 (2008).

26. Amar, L. *et al.* Succinate Dehydrogenase B Gene Mutations Predict Survival in Patients with Malignant Pheochromocytomas or Paragangliomas. *J. Clin. Endocrinol. Metab.* **92**, 3822–3828 (2007).

27. van Nederveen, F. H. *et al.* An immunohistochemical procedure to detect patients with paraganglioma and phaeochromocytoma with germline SDHB, SDHC, or SDHD gene mutations: a retrospective and prospective analysis. *Lancet Oncol.* **10**, 764–771 (2009).

28. Menara, M. *et al.* SDHD Immunohistochemistry: A New Tool to Validate *SDHx* Mutations in Pheochromocytoma/Paraganglioma. *J. Clin. Endocrinol. Metab.* **100**, E287–E291 (2015).

29. The NGS in PPGL (NGSnPPGL) Study Group *et al.* Consensus Statement on next-generation-sequencing-based diagnostic testing of hereditary phaeochromocytomas and paragangliomas. *Nat. Rev. Endocrinol.* **13**, 233–247 (2017).

30. Lam, A. K. Update on Adrenal Tumours in 2017 World Health Organization (WHO) of Endocrine Tumours. *Endocr. Pathol.* **28**, 213–227 (2017).

31. Mohammad Tavangar, S. *et al.* Immunohistochemical expression of Ki67, c-erbB-2, and c-kit antigens in benign and malignant pheochromocytoma. *Pathol. - Res. Pract.* **206**, 305–309 (2010).

32. Stenman, A., Zedenius, J. & Juhlin, C. The Value of Histological Algorithms to Predict the Malignancy Potential of Pheochromocytomas and Abdominal Paragangliomas—A Meta-Analysis and Systematic Review of the Literature. *Cancers* **11**, 225 (2019).

33. Roman-Gonzalez, A. & Jimenez, C. Malignant pheochromocytoma–paraganglioma: pathogenesis, TNM staging, and current clinical trials. *Curr. Opin. Endocrinol. Diabetes Obes.* **24**, 174–183 (2017).

34. Stenman, A., Zedenius, J. & Juhlin, C. C. Retrospective application of the pathologic tumor-node-metastasis classification system for pheochromocytoma and abdominal paraganglioma in a well characterized cohort with long-term follow-up. *Surgery* **166**, 901–906 (2019).

35. Turchini, J., Cheung, V. K. Y., Tischler, A. S., De Krijger, R. R. & Gill, A. J. Pathology and genetics of phaeochromocytoma and paraganglioma. *Histopathology* **72**, 97–105 (2018).

36. Hamidi, O. *et al.* Malignant Pheochromocytoma and Paraganglioma: 272 Patients Over 55 Years. *J. Clin. Endocrinol. Metab.* **102**, 3296–3305 (2017).

37. Huang, K.-H. *et al.* Clinical and pathological data of 10 malignant pheochromocytomas: Long-term follow up in a single institute: Long-term follow up of malignant pheochromocytoma. *Int. J. Urol.* **14**, 181–185 (2007).

38. Lee, J. H. *et al.* National Cancer Data Base report on malignant paragangliomas of the head and neck. *Cancer* **94**, 730–737 (2002).

39. Ayala-Ramirez, M. *et al.* Bone Metastases and Skeletal-Related Events in Patients With Malignant Pheochromocytoma and Sympathetic Paraganglioma. *J. Clin. Endocrinol. Metab.* **98**, 1492–1497 (2013).

40. Ayala-Ramirez, M. *et al.* Clinical Risk Factors for Malignancy and Overall Survival in Patients with Pheochromocytomas and Sympathetic Paragangliomas: Primary Tumor Size and Primary Tumor Location as Prognostic Indicators. *J. Clin. Endocrinol. Metab.* **96**, 717–725 (2011).

41. Shen, W. T., Sturgeon, C., Clark, O. H., Duh, Q.-Y. & Kebebew, E. Should pheochromocytoma size influence surgical approach? A comparison of 90 malignant and 60 benign pheochromocytomas. *Surgery* **136**, 1129–1137 (2004).

42. Parasiliti-Caprino, M. *et al.* Predictors of recurrence of pheochromocytoma and paraganglioma: a multicenter study in Piedmont, Italy. *Hypertens. Res.* (2019) doi:10.1038/s41440-019-0339-y.

43. Hescot, S. *et al.* Prognosis of Malignant Pheochromocytoma and Paraganglioma (MAPP-Prono Study): A European Network for the Study of Adrenal Tumors Retrospective Study. *J. Clin. Endocrinol. Metab.* **104**, 2367–2374 (2019).

44. Richards-Taylor, S. *et al.* The assessment of Ki-67 as a prognostic marker in neuroendocrine tumours: a systematic review and meta-analysis. *J. Clin. Pathol.* **69**, 612–618 (2016).

45. Kunz, P. L. *et al.* Consensus Guidelines for the Management and Treatment of Neuroendocrine Tumors: *Pancreas* **42**, 557–577 (2013).

46. Elder, E. E. *et al.* KI-67 AND hTERT Expression Can Aid in the Distinction between Malignant and Benign Pheochromocytoma and Paraganglioma. *Mod. Pathol.* **16**, 246–255 (2003).

47. Guadagno, E., D'Avella, E., Cappabianca, P., Colao, A. & Del Basso De Caro, M. Ki67 in endocrine neoplasms: to count or not to count, this is the question! A systematic review from the English language literature. *J. Endocrinol. Invest.* (2020) doi:10.1007/s40618-020-01275-9.

48. Moog, S. *et al.* Recurrence-Free Survival Analysis in Locally Advanced Pheochromocytoma: First Appraisal. *J. Clin. Endocrinol. Metab.* **106**, 2726–2737 (2021).

49. Brown, H. M., Komorowski, R. A., Wilson, S. D., Demeure, M. J. & Zhu, Y. R. Predicting metastasis of pheochromocytomas using DNA flow cytometry and immunohistochemical markers of cell proliferation: A positive correlation between MIB-1 staining and malignant tumor behavior. *Cancer* **86**, 1583–1589 (1999).

50. Kimura, N., Takekoshi, K. & Naruse, M. Risk Stratification on Pheochromocytoma and Paraganglioma from Laboratory and Clinical Medicine. *J. Clin. Med.* **7**, 242 (2018).

51. Koh, J.-M. *et al.* Validation of pathological grading systems for predicting metastatic potential in pheochromocytoma and paraganglioma. *PLOS ONE* **12**, e0187398 (2017).

52. Cho, Y. Y. *et al.* A clinical prediction model to estimate the metastatic potential of pheochromocytoma/paraganglioma: ASES score. *Surgery* **164**, 511–517 (2018).

53. Agarwal, A. *et al.* Size of the Tumor and Pheochromocytoma of the Adrenal Gland Scaled Score (PASS): Can They Predict Malignancy? *World J. Surg.* **34**, 3022–3028 (2010).

54. Taïeb, D. *et al.* Modern PET imaging for paragangliomas: Relation to genetic mutations. *Eur. J. Surg. Oncol. EJSO* **37**, 662–668 (2011).

55. Dong, Y. & Liu, Q. Differentiation of Malignant From Benign Pheochromocytomas With Diffusion-Weighted and Dynamic Contrast-Enhanced Magnetic Resonance at 3.0 T: *J. Comput. Assist. Tomogr.* **36**, 361–366 (2012).

56. Sahdev, A. & Reznek, R. Imaging evaluation of the non-functioning indeterminate adrenal mass. *Trends Endocrinol. Metab.* **15**, 271–276 (2004).

57. Fassnacht, M. *et al.* Management of adrenal incidentalomas: European Society of Endocrinology Clinical Practice Guideline in collaboration with the European Network for the Study of Adrenal Tumors. *Eur. J. Endocrinol.* **175**, G1–G34 (2016).

58. Rogowski-Lehmann, N. *et al.* Missed clinical clues in patients with pheochromocytoma/paraganglioma discovered by imaging. *Endocr. Connect.* **7**, 1168–1177 (2018).

59. Blake, M. A. *et al.* Low-density pheochromocytoma on CT: a mimicker of adrenal adenoma. *AJR Am. J. Roentgenol.* **181**, 1663–1668 (2003).

60. Caoili, E. M. *et al.* Adrenal Masses: Characterization with Combined Unenhanced and Delayed Enhanced CT. *Radiology* **222**, 629–633 (2002).

61. Park, J. J., Park, B. K. & Kim, C. K. Adrenal imaging for adenoma characterization: imaging features, diagnostic accuracies and differential diagnoses. *Br. J. Radiol.* **89**, 20151018 (2016).

62. Adam, S. Z. *et al.* Chemical Shift MR Imaging of the Adrenal Gland: Principles, Pitfalls, and Applications. *RadioGraphics* **36**, 414–432 (2016).

63. Taffel, M., Haji-Momenian, S., Nikolaidis, P. & Miller, F. H. Adrenal Imaging: A Comprehensive Review. *Radiol. Clin. North Am.* **50**, 219–243 (2012).

64. Thelen, J. & Bhatt, A. A. Multimodality imaging of paragangliomas of the head and neck. *Insights Imaging* **10**, 29 (2019).

65. Gimenez-Roqueplo, A.-P. *et al.* Imaging Work-Up for Screening of Paraganglioma and Pheochromocytoma in *SDHx* Mutation Carriers: A Multicenter Prospective Study from the PGL.EVA Investigators. *J. Clin. Endocrinol. Metab.* **98**, E162–E173 (2013).

66. Yuan, Y., Shi, H. & Tao, X. Head and neck paragangliomas: diffusion weighted and dynamic contrast enhanced magnetic resonance imaging characteristics. *BMC Med. Imaging* **16**, 12 (2016).

67. Neves, F. *et al.* Head and Neck Paragangliomas: Value of Contrast-Enhanced 3D MR Angiography. *Am. J. Neuroradiol.* **29**, 883–889 (2008).

68. Arsovic, E. *et al.* Quantitative biomarkers allow the diagnosis of head and neck paraganglioma on multiparametric MRI. *Eur. J. Radiol.* **143**, 109911 (2021).

69. Guichard, J.-P. *et al.* Morphological and functional imaging of neck paragangliomas. *Eur. Ann. Otorhinolaryngol. Head Neck Dis.* **134**, 243–248 (2017).

70. Hoegerle, S. *et al.* Pheochromocytomas: Detection with 18 F DOPA Whole-Body PET—Initial Results. *Radiology* **222**, 507–512 (2002).

71. Fottner, C. *et al.* 6-18F-fluoro-L-dihydroxyphenylalanine positron emission tomography is superior to 123I-metaiodobenzyl-guanidine scintigraphy in the detection of extraadrenal and hereditary pheochromocytomas and paragangliomas: correlation with vesicular monoamine transporter expression. *J. Clin. Endocrinol. Metab.* **95**, 2800–2810 (2010).

72. Taïeb, D. *et al.* Does iodine-131 meta-iodobenzylguanidine (MIBG) scintigraphy have an impact on the management of sporadic and familial phaeochromocytoma? *Clin. Endocrinol. (Oxf.)* **61**, 102–108 (2004).

73. van der Harst, E. *et al.* [(123)I]metaiodobenzylguanidine and [(111)In]octreotide uptake in begnign and malignant pheochromocytomas. *J. Clin. Endocrinol. Metab.* **86**, 685–693 (2001).

74. Pupilli, C. *et al.* Dopamine D2 receptor gene expression and binding sites in adrenal medulla and pheochromocytoma. *J. Clin. Endocrinol. Metab.* **79**, 56–61 (1994).

75. Timmers, H. J. L. M. *et al.* The Effects of Carbidopa on Uptake of 6-18F-Fluoro-L-DOPA in PET of Pheochromocytoma and Extraadrenal Abdominal Paraganglioma. *J. Nucl. Med.* **48**, 1599–1606 (2007).

76. Ilias, I. *et al.* Comparison of 6-18F-Fluorodopamine PET with 123I-Metaiodobenzylguanidine and 111In-Pentetreotide Scintigraphy in Localization of Nonmetastatic and Metastatic Pheochromocytoma. *J. Nucl. Med.* **49**, 1613–1619 (2008).

77. Timmers, H. J. L. M. *et al.* Use of 6-[18F]-fluorodopamine positron emission tomography (PET) as first-line investigation for the diagnosis and localization of non-metastatic and metastatic phaeochromocytoma (PHEO). *Clin. Endocrinol. (Oxf.)* **71**, 11–17 (2009).

78. Ilias, I. *et al.* Superiority of 6-[^{18} F]-Fluorodopamine Positron Emission Tomography *Versus* [^{131} I]-Metaiodobenzylguanidine Scintigraphy in the Localization of Metastatic Pheochromocytoma. *J. Clin. Endocrinol. Metab.* **88**, 4083–4087 (2003).

79. King, K. S. *et al.* Functional Imaging of *SDHx* -Related Head and Neck Paragangliomas: Comparison of ^{18} F-Fluorodihydroxyphenylalanine, ^{18} F-Fluorodopamine, ^{18} F-Fluoro-2-Deoxy- D

-Glucose PET, ^{123}I-Metaiodobenzylguanidine Scintigraphy, and ^{111}In-Pentetreotide Scintigraphy. *J. Clin. Endocrinol. Metab.* **96**, 2779–2785 (2011).

80. Pacak, K. *et al.* 6-[18F]Fluorodopamine Positron Emission Tomographic (PET) Scanning for Diagnostic Localization of Pheochromocytoma. *Hypertension* **38**, 6–8 (2001).

81. Noordzij, W. *et al.* Adrenal tracer uptake by 18F-FDOPA PET/CT in patients with pheochromocytoma and controls. *Eur. J. Nucl. Med. Mol. Imaging* **46**, 1560–1566 (2019).

82. Rufini, V. *et al.* Comparison of 123I-MIBG SPECT-CT and 18F-DOPA PET-CT in the evaluation of patients with known or suspected recurrent paraganglioma: *Nucl. Med. Commun.* **32**, 575–582 (2011).

83. Fiebrich, H.-B. *et al.* 6-[F-18]Fluoro-L-Dihydroxyphenylalanine Positron Emission Tomography Is Superior to Conventional Imaging with 123I-Metaiodobenzylguanidine Scintigraphy, Computer Tomography, and Magnetic Resonance Imaging in Localizing Tumors Causing Catecholamine Excess. *J. Clin. Endocrinol. Metab.* **94**, 3922–3930 (2009).

84. Luster, M. *et al.* Clinical value of 18F-fluorodihydroxyphenylalanine positron emission tomography/computed tomography (18F-DOPA PET/CT) for detecting pheochromocytoma. *Eur. J. Nucl. Med. Mol. Imaging* **37**, 484–493 (2010).

85. Imani, F. *et al.* 18F-FDOPA PET and PET/CT Accurately Localize Pheochromocytomas. *J. Nucl. Med.* **50**, 513–519 (2009).

86. Shulkin, B. L., Thompson, N. W., Shapiro, B., Francis, I. R. & Sisson, J. C. Pheochromocytomas: Imaging with 2-[Fluorine-18]fluoro-2-deoxy- D -glucose PET. *Radiology* **212**, 35–41 (1999).

87. Taieb, D. *et al.* 18F-FDG Avidity of Pheochromocytomas and Paragangliomas: A New Molecular Imaging Signature? *J. Nucl. Med.* **50**, 711–717 (2009).

88. Timmers, H. J. L. M. *et al.* Staging and Functional Characterization of Pheochromocytoma and Paraganglioma by 18F-Fluorodeoxyglucose (18F-FDG) Positron Emission Tomography. *JNCI J. Natl. Cancer Inst.* **104**, 700–708 (2012).

89. Timmers, H. J. L. M. *et al.* Comparison of 18F-Fluoro-L-DOPA, 18F-Fluoro-Deoxyglucose, and 18F-Fluorodopamine PET and 123I-MIBG Scintigraphy in the Localization of Pheochromocytoma and Paraganglioma. *J. Clin. Endocrinol. Metab.* **94**, 4757–4767 (2009).

90. Timmers, H. J. L. M. *et al.* Superiority of Fluorodeoxyglucose Positron Emission Tomography to Other Functional Imaging Techniques in the Evaluation of Metastatic *SDHB* -Associated Pheochromocytoma and Paraganglioma. *J. Clin. Oncol.* **25**, 2262–2269 (2007).

91. Favier, J. *et al.* The Warburg Effect Is Genetically Determined in Inherited Pheochromocytomas. *PLoS ONE* **4**, e7094 (2009).

92. Ueberberg, B. *et al.* Differential expression of the human somatostatin receptor subtypes sst1 to sst5 in various adrenal tumors and normal adrenal gland. *Horm. Metab. Res. Horm. Stoffwechselforschung Horm. Metab.* **37**, 722–728 (2005).

93. Reubi, J. C., Laissue, J., Krenning, E. & Lamberts, S. W. Somatostatin receptors in human cancer: incidence, characteristics, functional correlates and clinical implications. *J. Steroid Biochem. Mol. Biol.* **43**, 27–35 (1992).

94. Bustillo, A. *et al.* Octreotide scintigraphy in the head and neck. *The Laryngoscope* **114**, 434–440 (2004).

95. Schmidt, M. *et al.* Clinical value of somatostatin receptor imaging in patients with suspected head and neck paragangliomas. *Eur. J. Nucl. Med. Mol. Imaging* **29**, 1571–1580 (2002).

96. Koopmans, K. P. *et al.* 111In-octreotide is superior to 123I-metaiodobenzylguanidine for scintigraphic detection of head and neck paragangliomas. *J. Nucl. Med. Off. Publ. Soc. Nucl. Med.* **49**, 1232–1237 (2008).

97. Whiteman, M. L., Serafini, A. N., Telischi, F. F., Civantos, F. J. & Falcone, S. 111In octreotide scintigraphy in the evaluation of head and neck lesions. *AJNR Am. J. Neuroradiol.* **18**, 1073–1080 (1997).

98. Duet, M. *et al.* Clinical impact of somatostatin receptor scintigraphy in the management of paragangliomas of the head and neck. *J. Nucl. Med. Off. Publ. Soc. Nucl. Med.* **44**, 1767–1774 (2003).

99. Muros, M. A. *et al.* 111In-pentetreotide scintigraphy is superior to 123I-MIBG scintigraphy in the diagnosis and location of chemodectoma. *Nucl. Med. Commun.* **19**, 735–742 (1998).

100. Taïeb, D. *et al.* European Association of Nuclear Medicine Practice Guideline/Society of Nuclear Medicine and Molecular Imaging Procedure Standard 2019 for radionuclide imaging of phaeochromocytoma and paraganglioma. *Eur. J. Nucl. Med. Mol. Imaging* **46**, 2112–2137 (2019).

101. Janssen, I. *et al.* Superiority of [68Ga]-DOTATATE PET/CT to Other Functional Imaging Modalities in the Localization of SDHB-Associated Metastatic Pheochromocytoma and Paraganglioma. *Clin. Cancer Res.* **21**, 3888–3895 (2015).

102. Shahrokhi, P. *et al.* 68Ga-DOTATATE PET/CT Compared with 131I-MIBG SPECT/CT in the Evaluation of Neural Crest Tumors. *Asia Ocean. J. Nucl. Med. Biol.* (2019) doi:10.22038/aojnmb.2019.41343.1280.

103. Naji, M. *et al.* 68Ga-DOTA-TATE PET vs. 123I-MIBG in Identifying Malignant Neural Crest Tumours. *Mol. Imaging Biol.* **13**, 769–775 (2011).

104. Ilhan, H. *et al.* First-in-human 18F-SiFAlin-TATE PET/CT for NET imaging and theranostics. *Eur. J. Nucl. Med. Mol. Imaging* **46**, 2400–2401 (2019).

105. Ambrosini, V. *et al.* Consensus on molecular imaging and theranostics in neuroendocrine neoplasms. *Eur. J. Cancer* **146**, 56–73 (2021).

106. Amar, L. *et al.* International consensus on initial screening and follow-up of asymptomatic SDHx mutation carriers. *Nat. Rev. Endocrinol.* **17**, 435–444 (2021).

107. Fani, M., Nicolas, G. P. & Wild, D. Somatostatin Receptor Antagonists for Imaging and Therapy. *J. Nucl. Med.* **58**, 61S-66S (2017).

108. Jasim, S. & Jimenez, C. Metastatic pheochromocytoma and paraganglioma: Management of endocrine manifestations, surgery and ablative procedures, and systemic therapies. *Best Pract. Res. Clin. Endocrinol. Metab.* **34**, 101354 (2020).

109. Shamblin, W. R., ReMine, W. H., Sheps, S. G. & Harrison, E. G. Carotid body tumor (chemodectoma). *Am. J. Surg.* **122**, 732–739 (1971).

110. Department of Radiology, Christian Medical College, Vellore, India *et al.* Imaging criteria to predict Shamblin group in carotid body tumors – revisited. *Diagn. Interv. Radiol.* **27**, 354–359 (2021).

111. Arya, S., Rao, V., Juvekar, S. & Dcruz, A. K. Carotid Body Tumors: Objective Criteria to Predict the Shamblin Group on MR Imaging. *Am. J. Neuroradiol.* **29**, 1349–1354 (2008).

112. Prakash, P., Ramachandran, R., Tandon, N. & Kumar, R. Open surgery for pheochromocytoma: Current indications and outcomes from a retrospective cohort. *Indian J. Urol. IJU J. Urol. Soc. India* **36**, 21–25 (2020).

113. Amar, L. *et al.* Recurrence or new tumors after complete resection of pheochromocytomas and paragangliomas: a systematic review and meta-analysis. *J. Hypertens.* **34**, e269 (2016).

114. Kumar, R. M. *et al.* Canadian Urological Association Best Practice Report on the long-term followup for patients with pheochromocytomas. *Can. Urol. Assoc. J.* **13**, (2019).

115. Nölting *et al.* Current Management of Pheochromocytoma/Paraganglioma: A Guide for the Practicing Clinician in the Era of Precision Medicine. *Cancers* **11**, 1505 (2019).

116. Chrisoulidou, A., Kaltsas, G., Ilias, I. & Grossman, A. B. The diagnosis and management of malignant phaeochromocytoma and paraganglioma. *Endocr. Relat. Cancer* **14**, 569–585 (2007).

117. Roman-Gonzalez, A. *et al.* Impact of Surgical Resection of the Primary Tumor on Overall Survival in Patients With Metastatic Pheochromocytoma or Sympathetic Paraganglioma: *Ann. Surg.* **268**, 172–178 (2018).

118. Venkatesan, A. M., Locklin, J., Dupuy, D. E. & Wood, B. J. Percutaneous Ablation of Adrenal Tumors. *Tech. Vasc. Interv. Radiol.* **13**, 89–99 (2010).

119. Chien-Hsien Lo, Yeu-Sheng Tyan, & Kwo-Chang Ueng. Immediate Results and Long-Term Outcomes Following Percutaneous Radiofrequency Ablation of Unilateral Aldosterone-Producing Adenoma. *Acta Cardiol. Sin.* **36**, (2020).

120. Kohlenberg, J. *et al.* Efficacy and Safety of Ablative Therapy in the Treatment of Patients with Metastatic Pheochromocytoma and Paraganglioma. *Cancers* **11**, 195 (2019).

121. McBride, J. F. *et al.* Minimally Invasive Treatment of Metastatic Pheochromocytoma and Paraganglioma: Efficacy and Safety of Radiofrequency Ablation and Cryoablation Therapy. *J. Vasc. Interv. Radiol.* **22**, 1263–1270 (2011).

122. Gravel, G. *et al.* Prevention of serious skeletal-related events by interventional radiology techniques in patients with malignant paraganglioma and pheochromocytoma. *Endocrine* **59**, 547–554 (2018).

123. Eriksson, J. *et al.* Surgery and Radiofrequency Ablation for Treatment of Liver Metastases from Midgut and Foregut Carcinoids and Endocrine Pancreatic Tumors. *World J. Surg.* **32**, 930–938 (2008).

124. de Baère, T. *et al.* Radiofrequency ablation is a valid treatment option for lung metastases: experience in 566 patients with 1037 metastases. *Ann. Oncol.* **26**, 987–991 (2015).

125. Pacak, K. *et al.* Radiofrequency Ablation: a Novel Approach for Treatment of Metastatic Pheochromocytoma. *JNCI J. Natl. Cancer Inst.* **93**, 648–649 (2001).

126. Orditura, M. *et al.* Pancreatic neuroendocrine tumors: Nosography, management and treatment. *Int. J. Surg.* **28**, S156–S162 (2016).

127. Baère, T. de *et al.* Midterm Local Efficacy and Survival after Radiofrequency Ablation of Lung Tumors with Minimum Follow-up of 1 Year: Prospective Evaluation. *Radiology* **240**, 587–596 (2006).

128. Dromain, C. *et al.* Detection of Liver Metastases From Endocrine Tumors: A Prospective Comparison of Somatostatin Receptor Scintigraphy, Computed Tomography, and Magnetic Resonance Imaging. *J. Clin. Oncol.* **23**, 70–78 (2005).

129. Hellman, P., Ladjevardi, S., Skogseid, B., Åkerström, G. & Elvin, A. Radiofrequency Tissue Ablation Using Cooled Tip for Liver Metastases of Endocrine Tumors. *World J. Surg.* **26**, 1052–1056 (2002).

130. Venkatesan, A. M. *et al.* Radiofrequency Ablation of Metastatic Pheochromocytoma. *J. Vasc. Interv. Radiol.* **20**, 1483–1490 (2009).

131. Lee, E., Leon Pachter, H. & Sarpel, U. Hepatic Arterial Embolization for the Treatment of Metastatic Neuroendocrine Tumors. *Int. J. Hepatol.* **2012**, 1–8 (2012).

132. Takahashi, K. *et al.* Malignant Pheochromocytoma with Multiple Hepatic Metastases Treated by Chemotherapy and Transcatheter Arterial Embolization. *Intern. Med.* **38**, 349–354 (1999).

133. Watanabe, D. *et al.* Transcatheter Arterial Embolization for the Treatment of Liver Metastases in a Patient with Malignant Pheochromocytoma. *Endocr. J.* **53**, 59–66 (2006).

134. Hidaka, S. *et al.* Malignant Pheochromocytoma with Liver Metastasis Treated by Transcatheter Arterial Chemo-Embolization (TACE). *Intern. Med.* **49**, 645–651 (2010).

135. Mora, J., Cruz, O., Parareda, A., Sola, T. & de Torres, C. Treatment of disseminated paraganglioma with gemcitabine and docetaxel. *Pediatr. Blood Cancer* **53**, 663–665 (2009).

136. White, J. B., Link, M. J. & Cloft, H. J. Endovascular embolization of paragangliomas: A safe adjuvant to treatment. *J. Vasc. Interv. Neurol.* **1**, 37–41 (2008).

137. Michelozzi, C. *et al.* Arterial embolization with Onyx of head and neck paragangliomas. *J. NeuroInterventional Surg.* **8**, 626–635 (2016).

138. Jackson, R. S. *et al.* The Effects of Preoperative Embolization on Carotid Body Paraganglioma Surgery: A Systematic Review and Meta-analysis. *Otolaryngol. Neck Surg.* **153**, 943–950 (2015).

139. Wang, P. *et al.* Computerized Tomography Guided Percutaneous Ethanol Injection for the Treatment of Hyperfunctioning Pheochromocytoma. *J. Urol.* **170**, 1132–1134 (2003).

140. Suárez, C. *et al.* Jugular and vagal paragangliomas: Systematic study of management with surgery and radiotherapy. *Head Neck* **35**, 1195–1204 (2013).

141. Hinerman, R. W., Amdur, R. J., Morris, C. G., Kirwan, J. & Mendenhall, W. M. Definitive radiotherapy in the management of paragangliomas arising in the head and neck: A 35-year experience. *Head Neck* **30**, 1431–1438 (2008).

142. Vogel, J. *et al.* External Beam Radiation Therapy in Treatment of Malignant Pheochromocytoma and Paraganglioma. *Front. Oncol.* **4**, (2014).

143. Breen, W. *et al.* External beam radiation therapy for advanced/unresectable malignant paraganglioma and pheochromocytoma. *Adv. Radiat. Oncol.* **3**, 25–29 (2018).

144. Jimenez, C. Treatment for Patients With Malignant Pheochromocytomas and Paragangliomas: A Perspective From the Hallmarks of Cancer. *Front. Endocrinol.* **9**, 277 (2018).

145. Nomura, K. *et al.* Survival of Patients with Metastatic Malignant Pheochromocytoma and Efficacy of Combined Cyclophosphamide, Vincristine, and Dacarbazine Chemotherapy. *J. Clin. Endocrinol. Metab.* **94**, 2850–2856 (2009).

146. Huang, H. *et al.* Treatment of malignant pheochromocytoma/paraganglioma with cyclophosphamide, vincristine, and dacarbazine: Recommendation From a 22-Year Follow-up of 18 Patients. *Cancer* **113**, 2020–2028 (2008).

147. Niemeijer, N. D., Alblas, G., van Hulsteijn, L. T., Dekkers, O. M. & Corssmit, E. P. M. Chemotherapy with cyclophosphamide, vincristine and dacarbazine for malignant paraganglioma and pheochromocytoma: systematic review and meta-analysis. *Clin. Endocrinol. (Oxf.)* **81**, 642–651 (2014).

148. Averbuch, S. D. Malignant Pheochromocytoma: Effective Treatment with a Combination of Cyclophosphamide, Vincristine, and Dacarbazine. *Ann. Intern. Med.* **109**, 267 (1988).

149. Hadoux, J. *et al. SDHB* mutations are associated with response to temozolomide in patients with metastatic pheochromocytoma or paraganglioma: Temozolomide for Malignant Pheochromocytoma/Paraganglioma. *Int. J. Cancer* **135**, 2711–2720 (2014).

150. on behalf of the Spanish Cooperative Group of Neuroendocrine Tumors (GETNE) *et al.* Imaging approaches to assess the therapeutic response of gastroenteropancreatic neuroendocrine tumors (GEP-NETs): current perspectives and future trends of an exciting field in development. *Cancer Metastasis Rev.* **34**, 823–842 (2015).

151. Sundin, A., Garske, U. & Örlefors, H. Nuclear imaging of neuroendocrine tumours. *Best Pract. Res. Clin. Endocrinol. Metab.* **21**, 69–85 (2007).

152. IEO ENETS Center of Excellence for GEP NETs *et al.* Predictive Markers of Response to Everolimus and Sunitinib in Neuroendocrine Tumors. *Target. Oncol.* **12**, 611–622 (2017).

153. Dercle, L. *et al.* Using a single abdominal computed tomography image to differentiate five contrast-enhancement phases: A machine-learning algorithm for radiomics-based precision medicine. *Eur. J. Radiol.* **125**, 108850 (2020).

154. Hadoux, J. *et al.* Interferon-alpha Treatment for Disease Control in Metastatic Pheochromocytoma/Paraganglioma Patients. *Horm. Cancer* **8**, 330–337 (2017).

155. Joshua, A. M. *et al.* Rationale and Evidence for Sunitinib in the Treatment of Malignant Paraganglioma/Pheochromocytoma. *J. Clin. Endocrinol. Metab.* **94**, 5–9 (2009).

156. Ayala-Ramirez, M. *et al.* Treatment with Sunitinib for Patients with Progressive Metastatic Pheochromocytomas and Sympathetic Paragangliomas. *J. Clin. Endocrinol. Metab.* **97**, 4040–4050 (2012).

157. Baudin, E. *et al.* 567O First International Randomized Study in Malignant Progressive Pheochromocytoma and Paragangliomas (FIRSTMAPPP): An academic double-blind trial investigating sunitinib. *Ann. Oncol.* **32**, S621 (2021).

158. Martín-Richard, M. *et al.* Antiproliferative effects of lanreotide autogel in patients with progressive, well-differentiated neuroendocrine tumours: a Spanish, multicentre, open-label, single arm phase II study. *BMC Cancer* **13**, 427 (2013).

159. Wymenga, A. N. M. *et al.* Efficacy and Safety of Prolonged-Release Lanreotide in Patients With Gastrointestinal Neuroendocrine Tumors and Hormone-Related Symptoms. *J. Clin. Oncol.* **17**, 1111–1111 (1999).

160. Jimenez, C. *et al.* Use of the Tyrosine Kinase Inhibitor Sunitinib in a Patient with von Hippel-Lindau Disease: Targeting Angiogenic Factors in Pheochromocytoma and Other von Hippel-Lindau Disease-Related Tumors. *J. Clin. Endocrinol. Metab.* **94**, 386–391 (2009).

161. Naing, A. *et al.* Phase 2 study of pembrolizumab in patients with advanced rare cancers. *J. Immunother. Cancer* **8**, e000347 (2020).

162. Dercle, L. *et al.* Unconventional immune-related phenomena observed using 18F-FDG PET/CT in Hodgkin lymphoma treated with anti PD-1 monoclonal antibodies. *Eur. J. Nucl. Med. Mol. Imaging* **46**, 1391–1392 (2019).

163. Dercle, L. *et al.* ^{18} F-FDG PET and CT Scans Detect New Imaging Patterns of Response and Progression in Patients with Hodgkin Lymphoma Treated by Anti–Programmed Death 1 Immune Checkpoint Inhibitor. *J. Nucl. Med.* **59**, 15–24 (2018).

164. Dercle, L. *et al.* Kinetics and nadir of responses to immune checkpoint blockade by anti-PD1 in patients with classical Hodgkin lymphoma. *Eur. J. Cancer* **91**, 136–144 (2018).

165. Champiat, S. *et al.* Hyperprogressive Disease Is a New Pattern of Progression in Cancer Patients Treated by Anti-PD-1/PD-L1. *Clin. Cancer Res.* **23**, 1920–1928 (2017).

166. Dercle, L. *et al.* Nonsurgical giant cell tumour of the tendon sheath or of the diffuse type: Are MRI or 18F-FDG PET/CT able to provide an accurate prediction of long-term outcome? *Eur. J. Nucl. Med. Mol. Imaging* **42**, 397–408 (2015).

167. Ramos-Casals, M. *et al.* Immune-related adverse events of checkpoint inhibitors. *Nat. Rev. Dis. Primer* **6**, 38 (2020).

168. Liu, Y.-H. *et al.* Diagnosis and Management of Immune Related Adverse Events (irAEs) in Cancer Immunotherapy. *Biomed. Pharmacother.* **120**, 109437 (2019).

169. Mekki, A. *et al.* Detection of immune-related adverse events by medical imaging in patients treated with anti-programmed cell death 1. *Eur. J. Cancer* **96**, 91–104 (2018).

170. Goldfarb, L., Duchemann, B., Chouahnia, K., Zelek, L. & Soussan, M. Monitoring anti-PD-1-based immunotherapy in non-small cell lung cancer with FDG PET: introduction of iPERCIST. *EJNMMI Res.* **9**, 8 (2019).

171. van Hulsteijn, L. T., Niemeijer, N. D., Dekkers, O. M. & Corssmit, E. P. M. 131 I-MIBG therapy for malignant paraganglioma and phaeochromocytoma: systematic review and meta-analysis. *Clin. Endocrinol. (Oxf.)* **80**, 487–501 (2014).

172. Pryma, D. A. *et al.* Efficacy and Safety of High-Specific-Activity 131 I-MIBG Therapy in Patients with Advanced Pheochromocytoma or Paraganglioma. *J. Nucl. Med.* **60**, 623–630 (2019).

173. Jimenez, C., Erwin, W. & Chasen, B. Targeted Radionuclide Therapy for Patients with Metastatic Pheochromocytoma and Paraganglioma: From Low-Specific-Activity to High-Specific-Activity Iodine-131 Metaiodobenzylguanidine. *Cancers* **11**, 1018 (2019).

174. Gonias, S. *et al.* Phase II Study of High-Dose [^{131} I]Metaiodobenzylguanidine Therapy for Patients With Metastatic Pheochromocytoma and Paraganglioma. *J. Clin. Oncol.* **27**, 4162–4168 (2009).

175. Van Essen, M., Krenning, E. P., De Jong, M., Valkema, R. & Kwekkeboom, D. J. Peptide Receptor Radionuclide Therapy with radiolabelled somatostatin analogues in patients with somatostatin receptor positive tumours. *Acta Oncol.* **46**, 723–734 (2007).

176. Taïeb, D. & Pacak, K. Molecular imaging and theranostic approaches in pheochromocytoma and paraganglioma. *Cell Tissue Res.* **372**, 393–401 (2018).

177. Hope, T. A. *et al.* NANETS/SNMMI Procedure Standard for Somatostatin Receptor–Based Peptide Receptor Radionuclide Therapy with ^{177} Lu-DOTATATE. *J. Nucl. Med.* **60**, 937–943 (2019).

178. Imhof, A. *et al.* Response, Survival, and Long-Term Toxicity After Therapy With the Radiolabeled Somatostatin Analogue [^{90} Y-DOTA]-TOC in Metastasized Neuroendocrine Cancers. *J. Clin. Oncol.* **29**, 2416–2423 (2011).

179. Waldherr, C., Pless, M., Maecke, H. R., Haldemann, A. & Mueller-Brand, J. The clinical value of [90Y-DOTA]-D-Phe1-Tyr3-octreotide (90Y-DOTATOC) in the treatment of neuroendocrine tumours: A clinical phase II study. *Ann. Oncol.* **12**, 941–945 (2001).

180. Paganelli, G. *et al.* 90Y-DOTA-D-Phe1-Try3- octreotide in therapy of neuroendocrine malignancies. *Biopolymers* **66**, 393–398 (2002).

181. Esser, J. P. *et al.* Comparison of [177Lu-DOTA0,Tyr3]octreotate and [177Lu-DOTA0,Tyr3]octreotide: which peptide is preferable for PRRT? *Eur. J. Nucl. Med. Mol. Imaging* **33**, 1346–1351 (2006).

182. Prasad, V. *et al.* Lessons from a multicentre retrospective study of peptide receptor radionuclide therapy combined with lanreotide for neuroendocrine tumours: a need for standardised practice. *Eur. J. Nucl. Med. Mol. Imaging* (2020) doi:10.1007/s00259-020-04712-2.

183. Strosberg, J. *et al.* Phase 3 Trial of 177 Lu-Dotatate for Midgut Neuroendocrine Tumors. *N. Engl. J. Med.* **376**, 125–135 (2017).

184. Zovato, S. *et al.* Peptide Receptor Radionuclide Therapy (PRRT) with 177Lu-DOTATATE in Individuals with Neck or Mediastinal Paraganglioma (PGL). *Horm. Metab. Res.* **44**, 411–414 (2012).

185. Hope, T. A. *et al.* NANETS/SNMMI Consensus Statement on Patient Selection and Appropriate Use of 177Lu-DOTATATE Peptide Receptor Radionuclide Therapy. *J. Nucl. Med.* **61**, 222–227 (2020).

186. Goncalves, I. *et al.* Characteristics and outcomes of therapy-related myeloid neoplasms after peptide receptor radionuclide/chemoradionuclide therapy (PRRT/PRCRT) for metastatic neuroendocrine neoplasia: a single-institution series. *Eur. J. Nucl. Med. Mol. Imaging* **46**, 1902–1910 (2019).

187. Hescot, S. *et al.* One-Year Progression-Free Survival of Therapy-Naive Patients With Malignant Pheochromocytoma and Paraganglioma. *J. Clin. Endocrinol. Metab.* **98**, 4006–4012 (2013).

188. Grimaldi, S., Terroir, M. & Caramella, C. Advances in oncological treatment: limitations of RECIST 1.1 criteria. *Q. J. Nucl. Med. Mol. Imaging Off. Publ. Ital. Assoc. Nucl. Med. AIMN Int. Assoc. Radiopharmacol. IAR Sect. Soc. Of* **62**, 129–139 (2018).

189. Pinker, K., Riedl, C. & Weber, W. A. Evaluating tumor response with FDG PET: updates on PERCIST, comparison with EORTC criteria and clues to future developments. *Eur. J. Nucl. Med. Mol. Imaging* **44**, 55–66 (2017).

190. Werner, R. A. *et al.* Molecular imaging reporting and data systems (MI-RADS): a generalizable framework for targeted radiotracers with theranostic implications. *Ann. Nucl. Med.* **32**, 512–522 (2018).

191. Werner, R. A. *et al.* SSTR-RADS Version 1.0 as a Reporting System for SSTR PET Imaging and Selection of Potential PRRT Candidates: A Proposed Standardization Framework. *J. Nucl. Med.* **59**, 1085–1091 (2018).

192. Pedraza-Arévalo, S., Gahete, M. D., Alors-Pérez, E., Luque, R. M. & Castaño, J. P. Multilayered heterogeneity as an intrinsic hallmark of neuroendocrine tumors. *Rev. Endocr. Metab. Disord.* **19**, 179–192 (2018).

193. Carrasquillo, J. A. *et al.* Imaging of Pheochromocytoma and Paraganglioma. *J. Nucl. Med.* **62**, 1033–1042 (2021).

194. Aide, N., De Pontdeville, M. & Lopci, E. Evaluating response to immunotherapy with 18F-FDG PET/CT: where do we stand? *Eur. J. Nucl. Med. Mol. Imaging* **47**, 1019–1021 (2020).

195. Lamarca, A. *et al.* Value of Tumor Growth Rate (TGR) as an Early Biomarker Predictor of Patients' Outcome in Neuroendocrine Tumors (NET)—The GREPONET Study. *The Oncologist* **24**, (2019).

196. on behalf of the CLARINET Study Group *et al.* Tumor growth rate as a metric of progression, response, and prognosis in pancreatic and intestinal neuroendocrine tumors. *BMC Cancer* **19**, 66 (2019).

197. Mozley, P. D. *et al.* Measurement of Tumor Volumes Improves RECIST-Based Response Assessments in Advanced Lung Cancer. *Transl. Oncol.* **5**, 19–25 (2012).

198. Ctvrtlik, F. *et al.* Characteristic CT features of pheochromocytomas - probability model calculation tool based on a multicentric study. *Biomed. Pap.* **163**, 212–219 (2019).

199. Yi, X. *et al.* Adrenal incidentaloma: machine learning-based quantitative texture analysis of unenhanced CT can effectively differentiate sPHEO from lipid-poor adrenal adenoma. *J. Cancer* **9**, 3577–3582 (2018).

200. Yi, X. *et al.* Radiomics improves efficiency for differentiating subclinical pheochromocytoma from lipid-poor adenoma: a predictive, preventive and personalized medical approach in adrenal incidentalomas. *EPMA J.* **9**, 421–429 (2018).

201. Toriihara, A. *et al.* Prognostic value of somatostatin receptor expressing tumor volume calculated from 68Ga-DOTATATE PET/CT in patients with well-differentiated neuroendocrine tumors. *Eur. J. Nucl. Med. Mol. Imaging* **46**, 2244–2251 (2019).

202. Werner, R. A. *et al.* Pre-therapy Somatostatin Receptor-Based Heterogeneity Predicts Overall Survival in Pancreatic Neuroendocrine Tumor Patients Undergoing Peptide Receptor Radionuclide Therapy. *Mol. Imaging Biol.* **21**, 582–590 (2019).

203. Lussey-Lepoutre, C. *et al.* Succinate detection using in vivo 1H-MR spectroscopy identifies germline and somatic SDHx mutations in paragangliomas. *Eur. J. Nucl. Med. Mol. Imaging* **47**, 1510–1517 (2020).

204. Lussey-Lepoutre, C. *et al.* In Vivo Detection of Succinate by Magnetic Resonance Spectroscopy as a Hallmark of SDHx Mutations in Paraganglioma. *Clin. Cancer Res.* **22**, 1120–1129 (2016).

205. Varoquaux, A. *et al.* Magnetic resonance spectroscopy of paragangliomas: new insights into in vivo metabolomics. *Endocr. Relat. Cancer* **22**, M1–M8 (2015).

206. Richter, S. *et al.* Krebs Cycle Metabolite Profiling for Identification and Stratification of Pheochromocytomas/Paragangliomas due to Succinate Dehydrogenase Deficiency. *J. Clin. Endocrinol. Metab.* **99**, 3903–3911 (2014).

207. Letouzé, E. *et al.* SDH Mutations Establish a Hypermethylator Phenotype in Paraganglioma. *Cancer Cell* **23**, 739–752 (2013).

208. Ćwikła, J. B. *et al.* Circulating Transcript Analysis (NETest) in GEP-NETs Treated With Somatostatin Analogs Defines Therapy. *J. Clin. Endocrinol. Metab.* **100**, E1437–E1445 (2015).

209. Pavel, M. *et al.* NET Blood Transcript Analysis Defines the Crossing of the Clinical Rubicon: When Stable Disease Becomes Progressive. *Neuroendocrinology* **104**, 170–182 (2017).

210. Lin, D. *et al.* The Identification of Differentially Expressed Genes Showing Aberrant Methylation Patterns in Pheochromocytoma by Integrated Bioinformatics Analysis. *Front. Genet.* **10**, 1181 (2019).

211. Schreiner, F. & Beuschlein, F. Disease monitoring of patients with pheochromocytoma or paraganglioma by biomarkers and imaging studies. *Best Pract. Res. Clin. Endocrinol. Metab.* **34**, 101347 (2020).

212. Calsina, B. *et al.* Integrative multi-omics analysis identifies a prognostic miRNA signature and a targetable miR-21-3p/TSC2/mTOR axis in metastatic pheochromocytoma/paraganglioma. *Theranostics* **9**, 4946–4958 (2019).

213. Win, Z., Rahman, L., Murrell, J., Todd, J. & Al-Nahhas, A. The possible role of 68Ga-DOTATATE PET in malignant abdominal paraganglioma. *Eur. J. Nucl. Med. Mol. Imaging* **33**, 506–506 (2006).

214. Win, Z. *et al.* 68Ga-DOTATATE PET in neuroectodermal tumours: first experience. *Nucl. Med. Commun.* **28**, 359–363 (2007).

215. Ambrosini, V. *et al.* Comparison between 68Ga-DOTA-NOC and 18F-DOPA PET for the detection of gastro-entero-pancreatic and lung neuro-endocrine tumours. *Eur. J. Nucl. Med. Mol. Imaging* **35**, 1431–1438 (2008).

216. Wild, D. *et al.* DOTA-NOC, a high-affinity ligand of somatostatin receptor subtypes 2, 3 and 5 for labelling with various radiometals. *Eur. J. Nucl. Med. Mol. Imaging* **30**, 1338–1347 (2003).

217. Ambrosini, V. *et al.* 68Ga-DOTA-NOC PET/CT in comparison with CT for the detection of bone metastasis in patients with neuroendocrine tumours. *Eur. J. Nucl. Med. Mol. Imaging* **37**, 722–727 (2010).

218. Putzer, D. *et al.* Bone Metastases in Patients with Neuroendocrine Tumor: 68Ga-DOTA-Tyr3-Octreotide PET in Comparison to CT and Bone Scintigraphy. *J. Nucl. Med.* **50**, 1214–1221 (2009).

219. Kroiss, A. *et al.* Functional imaging in phaeochromocytoma and neuroblastoma with 68Ga-DOTA-Tyr3-octreotide positron emission tomography and 123I-metaiodobenzylguanidine. *Eur. J. Nucl. Med. Mol. Imaging* **38**, 865–873 (2011).

220. Yadav, D. *et al.* Evaluation of [68Ga]Ga-DATA-TOC for imaging of neuroendocrine tumours: comparison with [68Ga]Ga-DOTA-NOC PET/CT. *Eur. J. Nucl. Med. Mol. Imaging* **47**, 860–869 (2020).

221. Kratochwil, C. *et al.* SUV of [68Ga]DOTATOC-PET/CT Predicts Response Probability of PRRT in Neuroendocrine Tumors. *Mol. Imaging Biol.* **17**, 313–318 (2015).

222. Takada, K. *et al.* 18F-FDG uptake in PET/CT is a potential predictive biomarker of response to anti-PD-1 antibody therapy in non-small cell lung cancer. *Sci. Rep.* **9**, 13362 (2019).

223. Kim, H. S. *et al.* Prognostic Value of Volume-Based Metabolic Parameters Measured by (18)F-FDG PET/CT of Pancreatic Neuroendocrine Tumors. *Nucl. Med. Mol. Imaging* **48**, 180–186 (2014).

224. Seban, R.-D. *et al.* Prognostic and theranostic 18F-FDG PET biomarkers for anti-PD1 immunotherapy in metastatic melanoma: association with outcome and transcriptomics. *Eur. J. Nucl. Med. Mol. Imaging* **46**, 2298–2310 (2019).

225. Seban, R.-D. *et al.* Baseline metabolic tumor burden on FDG PET/CT scans predicts outcome in advanced NSCLC patients treated with immune checkpoint inhibitors. *Eur. J. Nucl. Med. Mol. Imaging* **47**, 1147–1157 (2020).

226. Wetz, C. *et al.* Predictive Value of Asphericity in Pretherapeutic [111In]DTPA-Octreotide SPECT/CT for Response to Peptide Receptor Radionuclide Therapy with [177Lu]DOTATATE. *Mol. Imaging Biol.* **19**, 437–445 (2017).

GABIACHE Gildas **2022-TOU3-1628**

THE ROLE OF IMAGE-GUIDED PRECISION MEDICINE IN THE DIAGNOSIS AND TREATMENT OF PHEOCHROMOCYTOMAS AND PARAGANGLIOMAS IN THE ERA OF IMAGING BIOMARKERS AND ARTIFICIAL INTELLIGENCE

Abstract :

Metastatic pheochromocytomas and paragangliomas are rare neural-crest-derived tumors with variable prognosis. In an era of tailored treatment strategies, medical imaging plays a crucial role in the surgeries, image-guided procedures, chemotherapies, immunotherapies and radionuclide therapies involved in the diagnosis and treatment of these tumors. Medical imaging helps to confirm the diagnosis, guide surgical resection, assess metastatic staging, and select patients for specific therapies. In this step-by-step review, we perform a comprehensive analysis of recent imaging modalities developed for pheochromocytomas and paragangliomas by covering their content and terminology as well as discussing the future implications of artificial intelligence.

Résumé :

Les phéochromocytomes et paragangliomes sont des tumeurs neuroendocrines rares dérivées des cellules de la crête neurale, dont le pronostic est variable. A l'ère des stratégies thérapeutiques adaptées au patient, les modalités d'imagerie modernes jouent un rôle central pour préparer la chirurgie, permettre des procédures de radiologie interventionnelle, évaluer la réponse sous chiomiothérapie, immunothérapie ou encore optimiser des thérapies vectorisées. Dans cette revue systématique, nous proposons une analyse compréhensive des modalités récentes d'imagerie d'intérêt pour les phéochromocytomes et paragangliomes, en abordant leurs principes, terminologies, et en discutant des futures implications de l'intelligence artificielle.

Mots-clés : Pheochromocytoma, paraganglioma, theranostic, image-guided therapies